THE PENNSYLVANIA STATE UNIVERSITY
SCHREYER HONORS COLLEGE

DEPARTMENT OF ENERGY & MINERAL ENGINEERING

Bioprospecting for Phosphorus Accumulating Organisms for Water Treatment

GABRIEL C. HIESTAND
SPRING 2023

A thesis
submitted in partial fulfillment
of the requirements
for a baccalaureate degree
in Environmental Systems Engineering
with honors in Environmental Systems Engineering

Reviewed and approved* by the following:

John Regan
Professor of Civil and Environmental Engineering
Thesis Supervisor

Jeremy Gernand
Associate Professor of Industrial Health and Safety
Honors Advisor

* Electronic approvals are on file

ABSTRACT

Nitrogen and phosphorus runoff into receiving waters creates a variety of harmful environmental challenges to vital aquatic ecosystems, most notably algal blooms. Phosphorus is an essential nutrient due to its role in food production, and depleted phosphorus reserves coupled with increasing global demand for food that is growing faster than phosphorus production presents a challenge that society must address. The use of phosphorus accumulating organisms (PAOs) during enhanced biological phosphorus removal (EBPR) presents an opportunity to both decrease algal blooms and recover phosphorus. In this study, bioprospecting was used to recover and identify PAOs present on rock biofilm samples taken from Spring Creek in Centre County, Pennsylvania. Cells were physically enriched using flow cytometry and DAPI staining, which imparts a yellow fluorescence emission when complexed with cells containing polyphosphate. The sorted cells enriched for PAO were cultured, and polymerase chain reaction (PCR) was used to amplify the 16S rRNA gene for sequencing. The Basic Local Alignment Search Tool (BLAST) was used to phylogenetically identify the isolated microbes based on their 16S rRNA gene sequences. Three colonies were cultured after flow cytometry, and BLAST results suggest that each of the colonies belonged to the genus *Pseudomonas*. Potential PAOs isolated were *P. chlororaphis* and *P. protegens* due to documented research of phosphorus metabolism and PHA catabolism, respectively. After DAPI staining of cells from the streak plates, each isolate was fluorescent using the yellow emission filter during fluorescence microscopy, suggesting that each of the isolates may have intracellular polyphosphate, even during continuously aerobic culturing conditions, and could be PAOs. Further research is required to confirm whether these microorganisms are indeed PAOs and if they are suitable for use during EBPR.

TABLE OF CONTENTS

LIST OF FIGURES

LIST OF TABLES

ACKNOWLEDGEMENTS

I'd like to thank Dr. Jay Regan and Dr. Jeremy Gernand for their support as my thesis supervisor and honors advisor, and even more for their shared wisdom and enthusiasm as mentors. Thanks to PhD candidates Olivia Rumble, Benjamin Castillo, and Patrick Hoover for their contributions. Thanks to Dr. Mani Rajeswaran and Desa Rae Abrams from the Huck Flow Cytometry Facility and Lucy Aplan and Ashley Price from the Huck Genomics Core Facility for their contributions to this work. I'd also like to express my gratitude to the Department of Energy and Mineral Engineering and the Department of Civil and Environmental Engineering at Penn State University for their support of my work. The opportunity to study at an institution with two departments that have environmental engineering focuses has provided me with a uniquely enriched perspective of the discipline. Thanks to the Schreyer Honors College for both providing me with this unique opportunity and for the consistent support throughout my undergraduate career during the highs and the lows. Thanks to Bevan Harbinson, my roommate of three years and fellow scholar with whom I've shared many late nights of thesis and other work. Without you, I doubt I could have maintained the attitude required to finish. Finally, I'd like to thank my family, specifically my parents Christopher and Jennifer and brother Mason, for their constant love and support during this endeavor and every other ambition I've ever had. I love you all.

Chapter 1

Introduction

Phosphorus is a vital nutrient for society due to its role in the production of the global food supply via fertilizer. Maintaining an adequate supply of phosphorus that meets the increasing global demand for food is therefore an essential task. Several factors will make this task difficult in the twenty first century. It is estimated that the global supply of phosphate will not meet the global demand by the year 2040, with the phosphate-scarce regions of South Asia, Latin America, the Caribbean, and Sub-Saharan Africa experiencing the most significant demand increases due to population growth. The same model estimates that the production of phosphate rock must double from 2020 levels by 2050 to meet demand (Nedelciu et al., 2020).

Economic factors coupled with these demand challenges add to the difficulties in securing food for the world's growing population. Globally, Morocco and the Western Sahara account for 71.5% of the known phosphate rock reserves, suggesting that only a few countries control the resources necessary for future growth (USGS, 2019). Between 2007 and 2008, the agricultural sector experienced an 800% price increase in phosphorus fertilizer prices due to a variety of socioeconomic and geopolitical factors. While there is uncertainty about the longevity of several of these factors, the industrial and scientific communities believe that the current phosphorus supply chain is unsustainable (Cordell & White, 2011).

In addition to the unsustainability of the phosphorus supply chain, there are significant detrimental environmental impacts associated with the current approach to phosphorus management. One of these environmental factors is eutrophication, which causes algal blooms. Since the 1980s, algal blooms have expanded in range and frequency in coastal areas, with one factor being increased nutrient runoff leading to eutrophication (Gobler, 2020).

During eutrophication, an increase in nitrogen and/or phosphorus concentrations provides necessary nutrients to support photosynthesis, leading to algal blooms. As the algae die, their decomposition depletes dissolved oxygen, creating anoxic “dead zones” that cannot support native aquatic species. At a large scale, dead zones can destroy vital marine ecosystems, including natural fisheries. Algal blooms also harm water quality by producing toxins and creating conditions that allow cyanobacteria to outcompete native microorganisms. Cyanobacteria pose public health risks for humans and livestock as the toxins they produce accumulate in water, and their toxins can harm larger marine populations. Outside of water quality and ecosystem degradation, the combined impacts of algal blooms negatively impact lucrative fishing, tourism, and recreation industries around the world (Chislock et al., 2013).

The scientific community predicts that algal blooms will increase in frequency and expand in range as a result of climate change. Climate change will increase the temperature, salinity, and carbon dioxide levels of bodies of water, all of which make them more suitable for algal bloom formation. In addition, extreme precipitation events will increase in frequency, as well periods of drought. Extreme precipitation events will increase the mass of nitrogen and phosphorus that runoff into bodies of water, increasing the severity of algal blooms. An extreme precipitation event caused an algal bloom in Iowa in 2011. Finally, sea level rise will increase areas of shallow and stable coastal water where algal blooms thrive (EPA).

One approach to reduce the spread of algal blooms to spread and stabilize future fertilizer supplies would be to treat water for phosphorus removal; and ideally recovery. Estimates suggest that 15-20% of the demand for phosphate rock could be reduced if phosphorus was recovered from domestic water streams (Yuan et al., 2012). One way to produce this outcome is by using microbes that metabolize polyphosphate, a group of microorganisms known as phosphate

accumulating organisms (PAOs). This defining characteristic of intracellular polyphosphate accumulation makes PAOs an appealing option for phosphate treatment in water.

Model PAOs have cyclic and interconnected anaerobic and aerobic metabolisms that give them a competitive growth advantage over other microbes (Figure 1). Under anaerobic conditions, PAOs take up and store carbon sources as polyhydroxyalkanoate (PHA) polymers, the production of which also requires energy in the form of adenosine triphosphate (ATP). In these conditions, ATP is formed from adenosine diphosphate (ADP) by hydrolyzing the polyphosphate accumulated during aerobic conditions. If PAOs run out of carbon storage accumulated from anerobic conditions, they must compete with other bacteria, but the ability to accumulate carbon during anaerobic conditions using stored polyphosphate allows PAOs to avoid competing with many other microorganisms during aerobic conditions. During aerobic conditions, PAOs uptake surplus phosphorus from their environment to create polyphosphate reserves and to convert ADP to ATP using the aerobic oxidation of the stored organics. ATP is used as an energy source for cell growth (Tarayre et al., 2016).

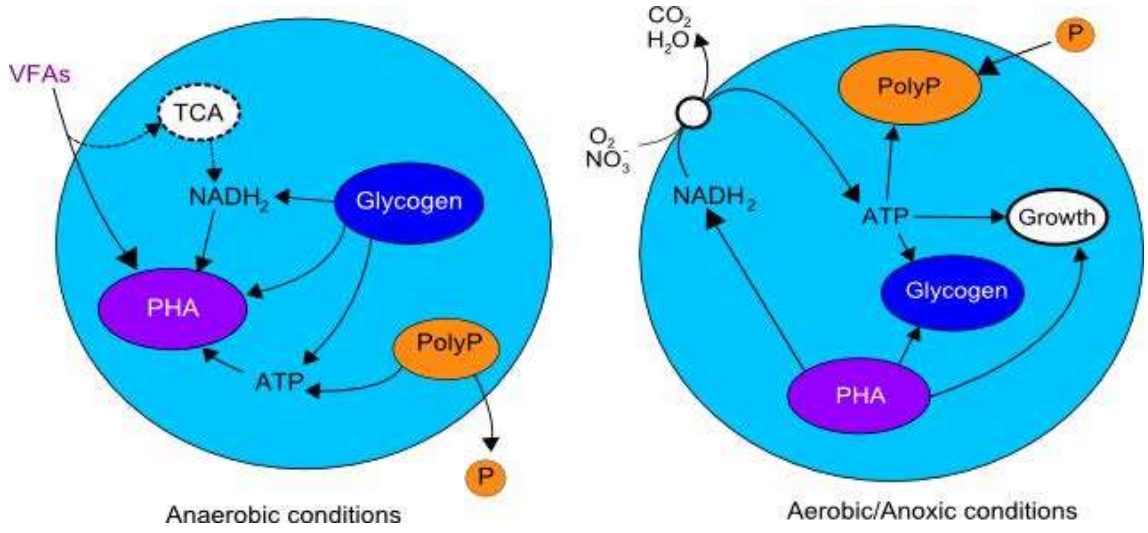

Figure 1. Schematic diagram of anaerobic and aerobic PAO metabolism (Yuan et al., 2012). TCA – tricarboxylic acid cycle, VFAs – volatile fatty acids, PHA – polyhydroxyalkanoates, PolyP – polyphosphate, P – orthophosphate, $NADH_2$ – nicotinamide adenine dinucleotide, ATP – adenosine triphosphate

PAOs are used in wastewater treatment in a microbial process called enhanced biological phosphorus removal (EBPR). EBPR produces sludge streams that are suitable for phosphorus recovery while producing effluent containing trace amounts of phosphorus. EBPR systems operate by subjecting the wastewater and suspended microbial biomass to alternating anaerobic and aerobic chambers. In the anerobic chamber, PAOs hydrolyze polyphosphate and release soluble phosphorus in support of carbon uptake and storage (Figure 1). Then, the influent and released phosphorus is removed in the aerobic phase when the PAOs accumulate polyphosphate. The PAOs are then wasted with the sludge or returned with activated sludge in a clarifier (Urdalen, 2013).

One important challenge in EBPR is the competition between glycogen accumulating organisms (GAOs) and PAOs. GAOs compete with PAOs for carbon sources in anaerobic conditions, and it is hypothesized that they can decrease the efficiency of EBPR systems over time in otherwise favorable conditions. GAOs are unwanted competition in EBPR due to their

similar organic storage metabolism to PAOs that is not accompanied by phosphorus removal (Oehmen et al., 2007). There is debate in the scientific community about the severity of the risk that GAOs pose to EBPR systems, at least partially because the first cases where GAOs were found to produce undesirable competition were anecdotal. Fully documented cases of GAOs impacting full-scale EBPR plants are scarce. Although GAOs have been found in several full-scale EBPR systems, they were operational with stable performance (Nielson et al., 2019).

Despite a lack of documentation of full-scale EBPR plants deteriorating in quality, research about the conditions where PAO growth is favored over GAO growth is useful for laboratory-scale research and for taking precautionary measures in full-scale plants. PAO metabolism has been found to be favored over GAO metabolism at a higher pH range (7.5-8.5), at a high carbon to phosphorus ratio (100 to 1), and when the carbon source is alternated between acetate and propionate in laboratory-scale EBPR reactors (Qingan et al., 2019; Lu et al., 2006).

Bioprospecting is the act of searching for novel microbes with a predetermined characteristic. Bioprospecting for PAOs is critical for their utilization in EBPR because a more complete knowledge of the available species of PAOs allows for possible improvements in the design of EBPR reactors, as novel phenotypic diversity may offer opportunities for enhancements in stability, carbon and phosphorus removal, and energy savings.

Several techniques for EBPR bioprospecting have been documented. Growing species found in EBPR sludge has been shown to produce cultivation bias because only certain species in EBPR sludges readily grow in laboratory conditions. Additionally, some of the species identified in this way do not display characteristics of PAOs. To eliminate cultivation bias, many in situ methods are used to identify PAOs. One way in which potential PAOs are detected is by polyphosphate staining techniques, usually by utilizing a dye and microscopy. Methylene Blue

and the fluorescent dye 4',6-DiAmidino-2-PhenylIndole dihydrochloride (DAPI) are frequently used to stain polyphosphate accumulation in cells. This dye staining method is frequently combined with fluorescence in situ hybridization (FISH), a technique involving fluorescently labeled oligonucleotide probes that can hybridize to complementary ribosomal RNA (rRNA) sequences in target microbes and allow their phylogenetic identification. An alternative to the FISH method is using fluorescence activated cell sorting (FACS), also referred to as flow cytometry, to quickly separate from a cell mixture the cells with a certain property, in this case polyphosphate stained with DAPI. The targeted cells can then be studied as potential PAOs (Günther, 2011).

Cells isolated for high polyphosphate concentration are often identified using the polymerase chain reaction (PCR) and 16S rRNA gene sequencing. PCR is an enzymatic method used to rapidly copy targeted fragments of genetic material of a given sample and the 16S rRNA gene is widely used to identify microbes (Johnson et al., 2019).

Previous bioprospecting has successfully isolated PAOs using DAPI staining and flow cytometry. In one study, wastewater sludge samples were stained with DAPI to target polyphosphate accumulation, targeted cells were isolated and recovered using FACS, and the isolated cells were identified using 16S rRNA gene sequencing. Another important finding was that approximately 70% of the isolated cells remained viable after DAPI staining and FACS, allowing for phenotypic validation of the methodology (Terashima et al., 2020).

Chapter 2

Background

The purpose of this study was to isolate and identify PAOs. DAPI staining and flow cytometry were used to sort cells containing significant concentrations of polyphosphate. The putative polyphosphate-containing sorted cells were cultured and then identified using PCR and 16S rRNA gene sequencing. Fluorescence microscopy was used before flow cytometry to verify yellow staining of intracellular polyphosphate granules and after 16S rRNA gene sequencing to observe the microbes. The primary goals were to verify this technique of PAO isolation following DAPI staining, identify the PAOs present at the selected environmental site, and potentially recover novel PAO isolates.

Most literature on PAOs focuses on their functionality in lab-scale EBPR reactors, determining conditions where they outcompete GAOs, and identifying the PAOs present in sludge. Few studies investigate PAOs present in the natural environment or their viability after DAPI staining. Identifying PAOs present in the environment reveals which PAOs outcompete various organisms in the central Pennsylvania region, and recovering novel isolates would allow the characterization of phenotypic diversity among microbes with the ability to store phosphate.

The microbes for this study were collected from Spring Creek, located in Centre County, Pennsylvania. The location of collection was adjacent to the SGL 333 Parking off of Shiloh Road, just downstream of the Benner Spring State Fish Hatchery. The coordinates of this location are 40º51’37.8”N, 77º48’32.6”W.

Chapter 3

Methods and Materials

Collection of the microorganisms for the study occurred at 40º51’37.8”N, 77º48’32.6”W, where microbes were collected from Spring Creek, in Centre County, Pennsylvania. Two rocks from the stream were collected for study: one bigger rock (BR) and one smaller rock (LR). In the lab, each rock was scraped to recover biofilm samples. A 1 mg/mL stock solution of DAPI was prepared in distilled water. Three 1-mL samples of microbes from each rock were prepared, one unstained control, one DAPI-stained sample that was not shredded, and one experimental sample from each rock. The experimental sample was shredded one hundred times in a syringe with a 22-gauge needle to break up flocs in the biofilm. To stain the DAPI stained control and experimental samples, the 1 mg/mL DAPI stock solution was diluted to 10 µg/mL. The DAPI stained control and experimental samples were stained with 1 mL of the diluted DAPI solution. The samples stained for 30 minutes in darkness at room temperature.

After DAPI staining, all samples were examined using bright field and epifluorescence microscopy to qualitatively confirm that the staining and biofilm disruption were successful and that an adequate number of individual cells were present in the experimental samples that could be isolated during flow cytometry. The samples were examined by preparing 0.1 µL of each sample on a slide for observation on the microscope. The control, DAPI stained control, and experimental sample from each rock made six examined samples total.

The experimental samples were placed in the flow cytometer at the Huck Flow Cytometry Facility in the Millennium Science Complex at Penn State University. During flow cytometry, two gates were used, a 355 nm laser with an emission band from 448-459 nm to

target DAPI-stained DNA and a 405 nm laser with an emission band from 546-620 nm to target DAPI-stained polyphosphate.

The cells from each sample sorted during flow cytometry were cultured with the medium used by Luo et al., 2021, modified with acetate serving as the electron donor. The medium was comprised of 0.15 L Solution A, 2.0 mL of trace metals, and 0.85 L of Solution B (Appendix A). The agar concentration was 15 g/L. Solution A contained 1.02 g/L of ammonium chloride, 0.01 g/L of peptone, 0.01 g/L of yeast extract, 1.2 g/L of magnesium sulfate heptahydrate, 0.19 g/L of calcium chloride monohydrate, and 11.33 g/L of sodium acetate trihydrate (The sodium acetate trihydrate is not present in the Luo et al., 2021 feed.). The trace metals solution contained 0.9 g/L of iron (III) chloride, 0.15 g/L of boric acid, 0.03 g/L of copper sulfate heptahydrate, 0.18 g/L of potassium iodide, 0.12 g/L of magnesium chloride tetrahydrate, 0.06 g/L of sodium molybdate, 0.12 g/L of zinc sulfate heptahydrate, 0.15 g/L of cobalt chloride hexahydrate, and 11.5 g/L of disodium ethylenediaminetetraacetic acid (EDTA). Solution B contained 0.132 g/L dipotassium phosphate and 0.103 g/L monopotassium phosphate. Sorted cell fractions were diluted prior to spread plating using phosphate-buffered saline solution (PBS) (Appendix A). The PBS contained 8.0 g/L of sodium chloride, 0.2 g/L of potassium chloride, 1.42 g/L of disodium phosphate, and 0.24 g/L of monopotassium phosphate. The pH of the PBS was adjusted to 7.35.

Several combinations of buffer and isolated cells were plated using the spread plating technique. The total volume spread on each plate was 100 µL. The plates were incubated at 25ºC for 10 days. Colonies appeared on three of the plates, all from LR. Two of the plates contained 100 µL of the isolated cells, and one plate contained 50 µL of the PBS buffer and 50µL of the isolated cells. To preserve the colonies and increase the number of cells available for study, each

colony was plated twice using the streak plating technique onto more of the 1.5% agar plates, making six streak plates total. The plates were incubated at 25 25ºC for 2 days.

After the incubation, the three isolates were phylogenetically identified using the polymerase chain reaction (PCR) to target the 16S rRNA gene. To prepare the samples for PCR, 60 µL of Promega PCR Master Mix (Promega M7502) was combined with 4.8 µL each of primers 8f and 1942r and 50.4 µL of distilled water (Appendix A). Promega M7502 is a 2X solution containing Taq DNA polymerase, dNTPs, magnesium chloride, and a reaction buffer. This solution was divided evenly into three tubes, and cells from each of the three colonies on spread plates were added to them. The tubes were placed inside a PCR thermal cycler for 30 cycles.

Gel electrophoresis was used to verify the successful amplification of the 16S rRNA gene in PCR. The gel was prepared using 0.5 g of agarose, 20 mL of Tris-acetate-EDTA (TAE), 5 µL of 10,000X SYBR safe DNA stain, and distilled water until the total volume was 50 mL (Appendix A). The gel was microwaved for 30 seconds to dissolve the components. A buffer used for the gel electrophoresis tray was prepared using 50 mL of 1% agarose, 20 mL TAE, and distilled water until the total volume of the solution was 1,000 mL (see Appendix A). The platform of the gel electrophoresis apparatus was then covered with the TAE buffer solution. Five wells in the gel were used: lanes 2-4 for the PCR products, and lanes 1 and 5 for 1 Kb Plus DNA Ladder. A 10X gel loading buffer containing glycerol to aid the DNA in sinking into the gel was also used. To prepare for gel electrophoresis, 1 µL of the 1 Kb Plus DNA Ladder or 5 µL PCR product and 1 µL of the 10X gel loading were mixed and pipetted in each well. The gel was subjected to 100 V for 45 minutes. After the time had elapsed, the gel was removed from the apparatus and an image was taken on a gel imaging system to determine if the 16S rRNA gene

was successfully amplified based on the expected result of approximately 1,500 base pairs for primers 8f and 1492r.

The 16S rRNA gene amplified by PCR was used for individual Sanger sequencing to identify the isolates. To measure the initial concentration of DNA template, 1 µL of each PCR product was placed on a NanoDrop One Microvolume UV-Vis Spectrophotometer. The concentration of DNA template for each isolate was diluted to the 40 ng/µL needed for individual Sanger sequencing using nuclease-free water. For individual Sanger sequencing, 5 µL of each diluted DNA template solution and 5 µL of primer (1 µM) per DNA template solution were required. The DNA templates and primers were sent to the Huck Institute Genomics Core Facility at Penn State University for individual Sanger sequencing.

The sequencing results were analyzed using Molecular Evolutionary Genetics Analysis (MEGA) software (MEGA-X). After trimming the sequence ends to only include high-quality sequence, the Basic Local Alignment Search Tool (BLAST) was used to find local regions of similarity between the isolate sequences and deposited sequences of known microorganisms.

To investigate the accumulation of polyphosphate in the isolated microbes, they were stained with DAPI and examined using eifluorescence microscopy. The DAPI stain was prepared by creating a 1 mg/mL DAPI stock solution that was diluted to 100 µg/mL in the same way as the previously described DAPI staining, however the final DAPI concentration was an order of magnitude larger. A volume of 1 mL of the diluted 100 µg/mL DAPI solution was used to stain cells collected from both streak plates for each of the three isolates. Cells were added to each DAPI staining solution using aseptic technique. Once the cells were added, staining occurred for 30 minutes in darkness and room temperature. The isolated microbes were examined by preparing 0.1 µL of each sample on a slide for observation on the microscope. The stained cells

were visualized using epifluorescence with an ultraviolet excitation filter and a yellow emission filter.

Chapter 4

Results

The samples of biofilm scraped from both rocks were examined using bright field microscopy to check for the presence of cells and the qualitative effectiveness of cell aggregate disruption for the experimental sample. Figures 2 and 3 show images taken after DAPI staining of both the cell aggregates and dispersed cells present after shredding respectively.

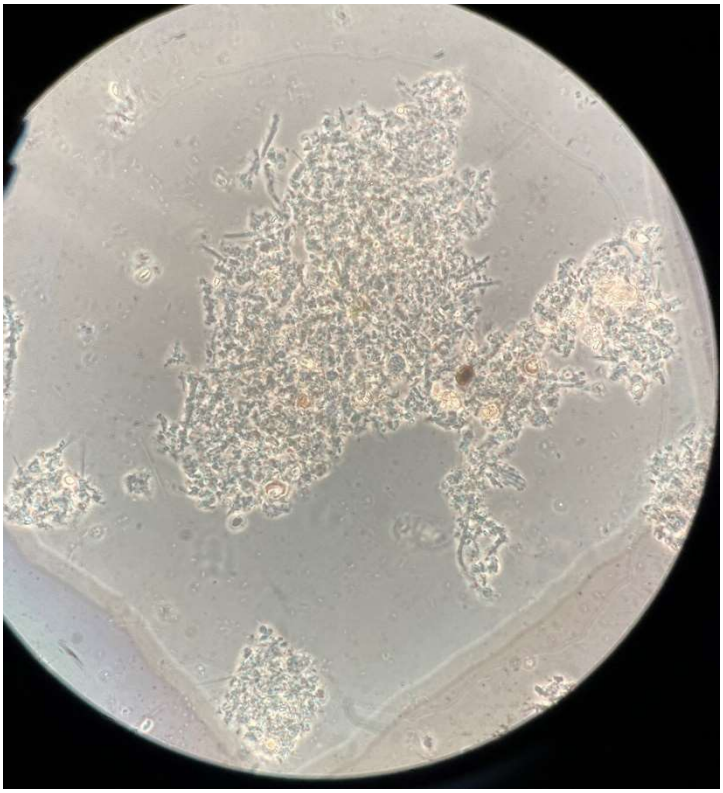

Figure 2. Brightfield image of biofilm cells scraped from rocks.

Figure 3. Biofilm experimental cells after disruption through syringe needle

Based on detection of yellow DAPI-polyphosphate fluorescence, flow cytometry isolated 175,685 cells from the disrupted experimental sample taken from LR, or about 6% of the total DAPI-stained cells in this sample and 175,295 cells from the experimental sample taken from BR, or about 3%, of the total cells in this sample. Figures 4 and 5 show dot plots of DAPI-conferred DNA fluorescence versus DAPI-polyphosphate fluorescence for LR and BR samples, respectively. The cell sorting gate for each sample is outlined on the corresponding figure, showing the discrimination of particles with disproportionately high DAPI-polyphosphate intensity relative to the DAPI-DNA signal.

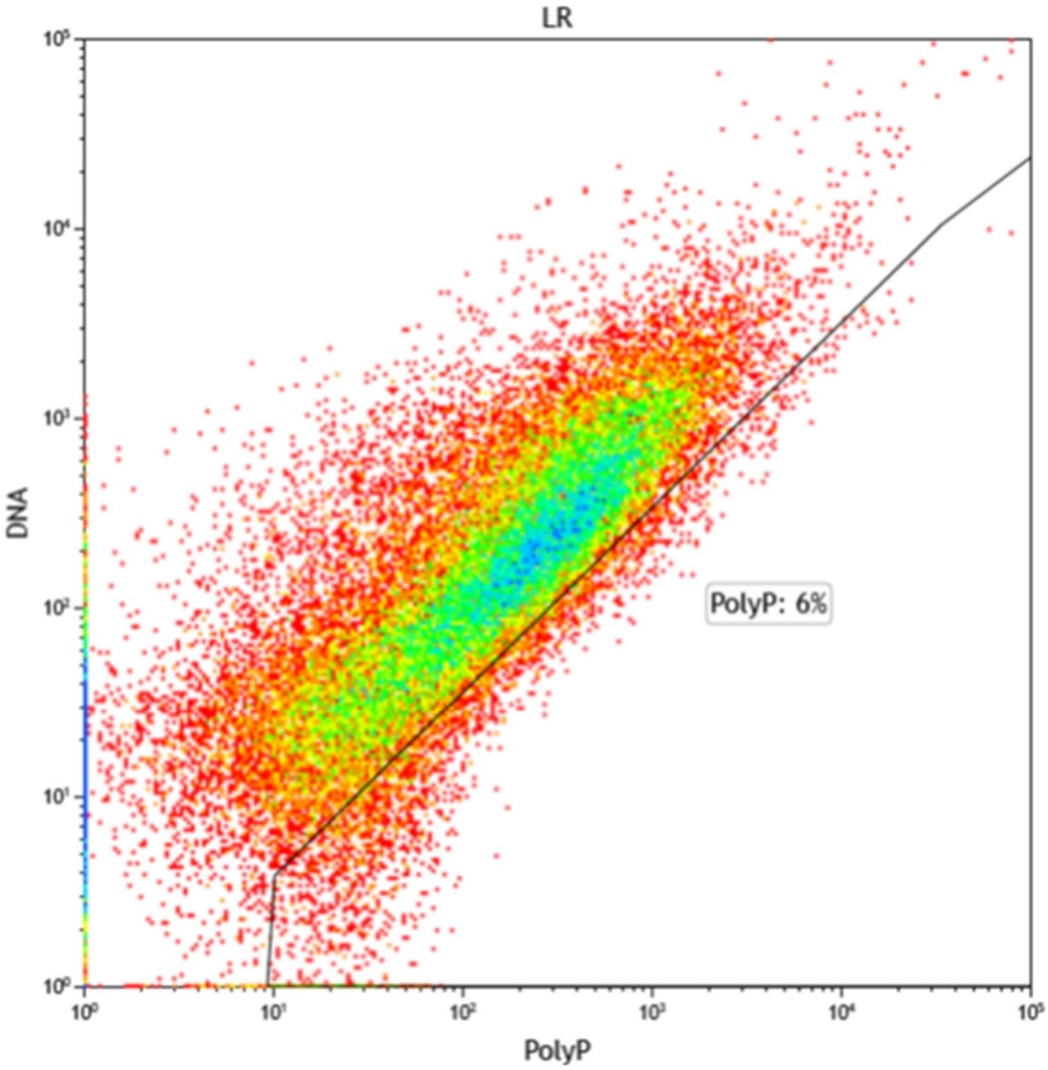

Figure 4. Flow cytometry dot plot for LR, showing DNA fluorescence vs. polyphosphate fluorescence. The cell sorting gate is delineated in the bottom right.

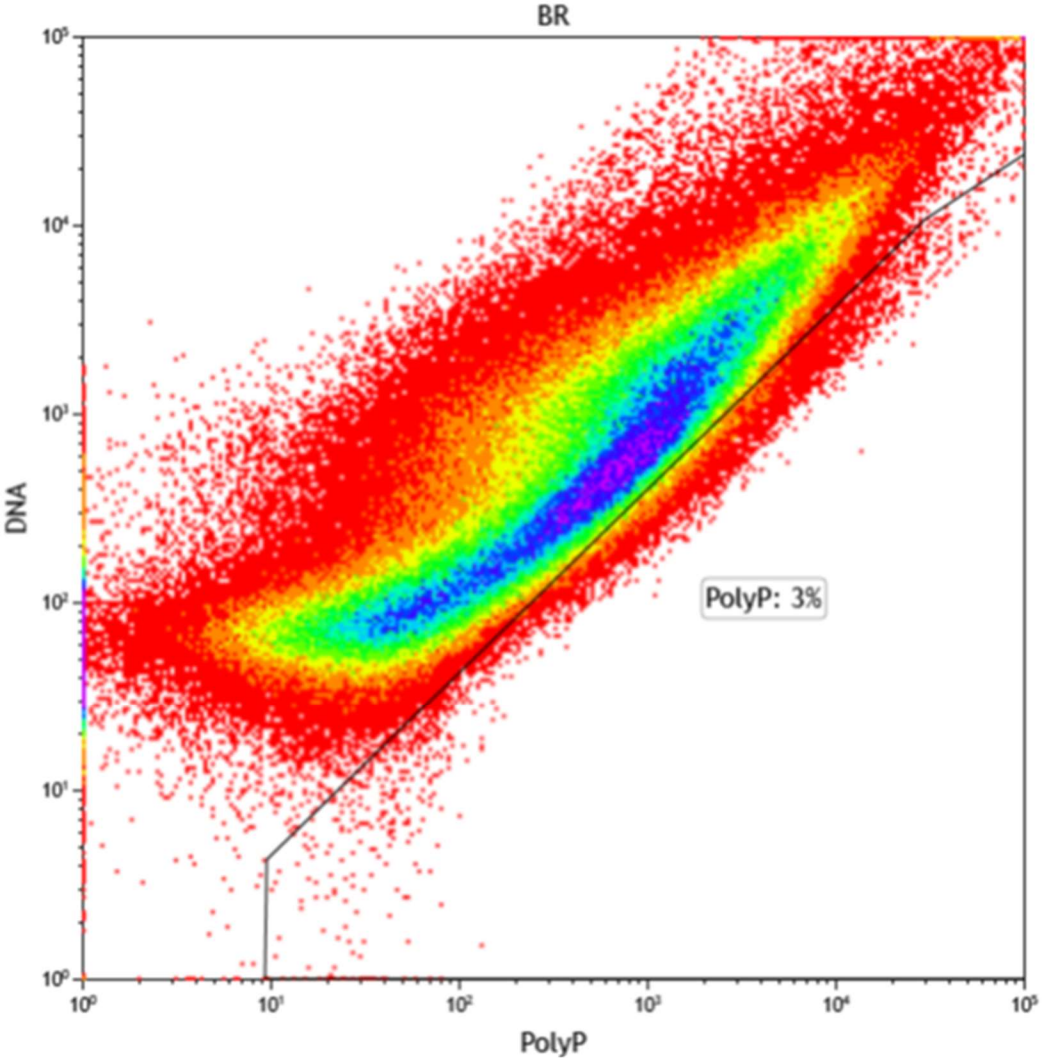

Figure 5. Flow cytometry dot plot for BR, showing DNA fluorescence vs. polyphosphate fluorescence. The cell sorting gate is delineated in the bottom right.

Spread plating yielded a colony on three of the agar plates, each from LR. The first two colonies, LR1 (Figure 6) and LR2 (Figure 7), grew on plates that contained 100 µL of the cells isolated from flow cytometry. The third colony, LR3 (Figure 8), grew on a plate that contained 50 µL of the PBS buffer and 50µL of the cells isolated from flow cytometry. Cells from each of these colonies were transferred to two separate 1.5% agar plates per colony using the streak plating technique (Appendix B).

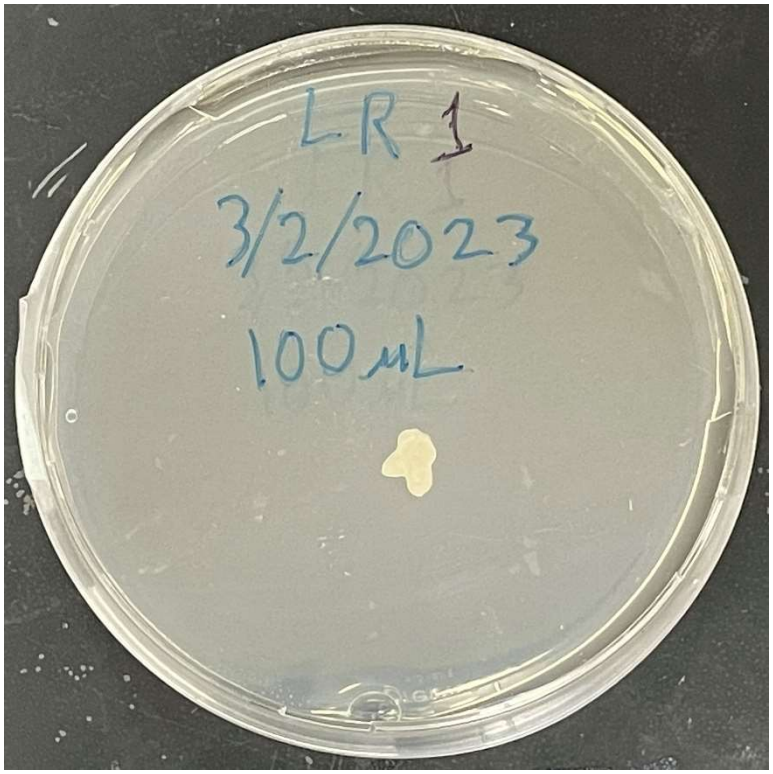

Figure 6. LR1 colony growing on the acetate-based medium.

Figure 7. LR2 colony growing on the acetate-based medium.

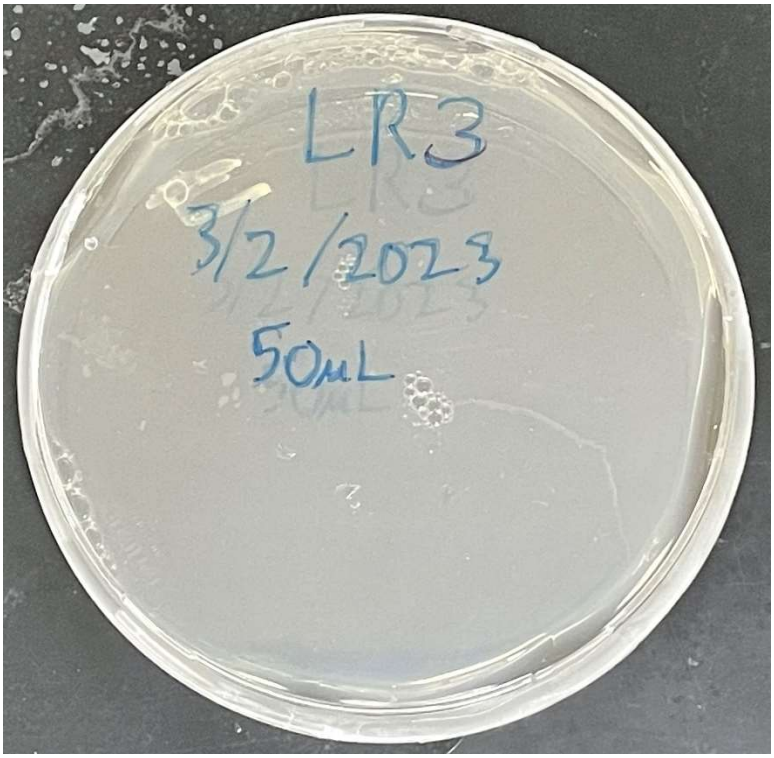

Figure 8. LR3 colony growing on the acetate-based medium.

Gel electrophoresis was used to determine if amplification of the 16S rRNA gene using the 8f and 1492r primers was successful. Figure 9 shows the 1 Kb Plus DNA Ladder bands on either side of the bands produced from PCR of each of the three colonies.

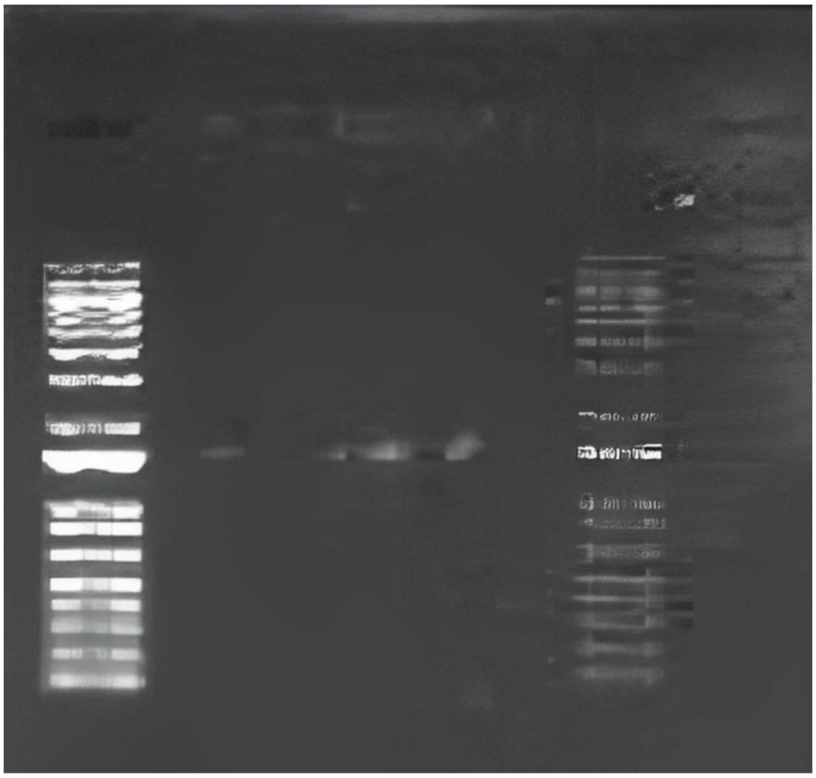

Figure 9. Gel electrophoresis showed bands approximately 1.500 bp from LR1 (Lane 2), LR2 (Lane 3), and LR3 (Lane 4).

Sequencing yielded a high-quality region for each combination of DNA template and primer (Appendix C). The BLAST results reported several species of microorganisms that had a high percentage identity match with sequences from the LR1, LR2, and LR3 isolates. Each BLAST result with a high percentage match was of the genus *Pseudomonas*, but the species varied across the different samples (Appendix D).

The LR1A sample was sequenced using the 1492r primer, which produced a high-quality sequence of 275 consecutive base pairs. This sequence was 96.70% identical to the 16S rRNA gene sequencing of microorganism *P. chengduensis*. This bacterium is a short rod and was isolated from a solid-waste disposal site in Chengdu, Sichuan, China. *P. chengduensis* is gram-negative, non-motile, non-flagellated, and non-sporulating. It is nitrate reducing, and can reduce

a variety of metals, including iron (III), manganese (II), copper (II), nickel (II), cadmium (II), cobalt (II), aluminum (III), selenium (IV), and tellurium (IV) under aerobic conditions. *P. chengduensis* can grow in a temperature range of 4 – 41 ºC, a pH range of 6 – 10, and in the presence of 0-8% sodium chloride. It is positive for catalase, oxidase, arginine dihydrolase, gelatin liquefaction, and production of hydrogen sulfide and indole. It is also positive for the utilization of D-fucose, L-serine, D-fructose, L-alanine, L-arginine, L-glutamic acid, L-histidine, L-pyroglutamic acid, L-lactic acid, citric acid, L-malic acid, propionic acid, γ-aminobutryric acid, acetic acid, α-ketoglutaric acid, D-salicin, α-D-glucose, glycyl L-proline, L-aspartic acid, pectin, D-galacturonic acid, L-galactonic acid lactone, D-gluconic acid, D-glucuronic acid, glucuronamide, mucic acid, D-saccharic acid, methyl pyruvate, bromosuccinic acid, acetoacetic acid and formic acid as carbon sources (Tao et al., 2014). This truncated LR1A sequence was 96.70% identical to that of *P. tolaasii*. This gram-negative species has been isolated on mushroom farms and is known for producing the toxin tolaasin, which causes brown blotch disease in mushrooms. *P. tolaasii* has been found to grow in laboratory setting at a temperature of 25 ºC (Godfrey et al., 2001). The LR1A sequence was 96.34% identical to that of *P. chlororaphis*, a gram-negative, aerobic nitrifier that is antagonistic to soil-borne plant pathogens and forms biofilms in plant root ecosystems. Additionally, some isolates of *P. chlororaphis* have been shown to metabolize phosphate (Anderson & Kim, 2020).

The LR1B sample was sequenced using the 8f primer, which produced a high-quality sequence of 186 consecutive base pairs. This sequence was 97.83% identical to that of *P. protegens*. This species has been shown to depolymerize lignin and grow on polyhydroxybutyrate (PHB) and polyhydroxyoctanoate (PHO), and some isolates have genes associated with PHA catabolism (Rodríguez et al., 2022). This LR1B sequence was 97.83%

identical to that of *P. veronii*, a gram-negative species often isolated in mineral water that grows at temperatures of 4 – 36 ºC and has one polar flagellum. This species is oxidase, catalase, and arginine dihydrolase positive and grows on α-aminobutyrate, D-xylose, L-arabinose, D-mannose, D-galactose, sucrose, butyrate, isobutyrate, erythritol, sorbitol, inositol, D-alanine, L-tryptophan, and trigonelline as the sole source of carbon and energy (Elomari et al., 1996). The LR1B sequence was 97.83% identical to the 16S rRNA gene sequence of *P. extremorientalis*, a species previously isolated from mineral water. *P. extremorientalis* is a chemo-organotroph with a respiratory metabolism that oxidizes dextrin, glycogen, Tween 40, Tween 80, N-acetyl-D-glucosamine, adonitol, L-arabinose, D-arabitol, cellobiose, D-fructose, D-galactose, m-inositol, α-lactose, α-D-lactose lactulose, maltose, D-mannitol, D-mannose, D-methyl glucoside, psicose, D-sorbitol, sucrose, D-trehalose, tyranose, xylitol, methyl pyruvate, mono-methyl succinate, acetic acid, cisaconitic acid, citric acid, formic acid, D-galactonic acid γ-lactone, D-galacturonic acid, D-gluconic acid, D-glucosaminic acid, D-clucuronic acid, α-hydroxybutyric acid, β-hydroxybutyric acid, γ-hydroxybutyric acid, itaconic acid, 2-oxobutyric acid, 2-oxoglutaric acid, 2-oxovaleric acid, DL-lactic acid, malonic acid, propionic acid, quinic acid, D-saccharic acid, sebacic acid, succinic acid, bromosuccinic acid, succinamic acid, glucuronamide, alaninamide, D-alanine, L-alanine, L-alanyl-glycine, L-asparagine, L-aspartic acid, L-glutamic acid, glycyl-L-aspartic acid, glycyl-L-glutamic acid, L-histidine, L-leucine, L-proline, L-pyroglutamic acid, D-serine, L-serine, L-threonine, DL-camitine, γ-aminobutyric acid, urocanic acid, inosine, uridine, thymidine, 2-aminoethanol, glycerol, α- DL-glycerol phosphate, and glucose 1-phosphate (Ivanova et al., 2002).

The LR2A sample was sequenced using the 1492r primer, which produced a high-quality sequence of 566 consecutive base pairs. This sequence was 100% identical to that of *P.*

fluorescens, a gram-negative rod-shaped microbe with polar flagella. *P. fluorescens* can grow under aerobic conditions in a sodium chloride concentration of up to 3.0%, in a temperature range between 5 – 30 ºC, and in a pH range from 5.0 – 8.5. This species is catalase positive, a nitrifier, and grows in Koser's citrate medium. For its metabolism, *P. fluorescens* can utilize glucose, galactose, fructose, maltose, 1-malic acid or lactic acid as its sole added carbon source in a Koser-type inorganic salt medium (Rhodes, 1959). The LR2A sequence was also 100% identical to *P. fildesensis*, a microbe that has been isolated in Antarctic soil. *P. fildesensis* is a gram-negative, rod-shaped bacterium with one or multiple polar or peritrichous flagella. It grows aerobically and anaerobically only in the presence of nitrate, can grow in a temperature range of 4 – 30 ºC, grows in up to 4% sodium chloride and is positive for catalase (Pavlov et al., 2020). The LR2A sequence was also 100% identical to *P. veronii*, which was previously described for LR1B.

The LR2B sample was sequenced using the 8f primer, which produced a high-quality sequence of 190 consecutive base pairs. This LR2B sequence was 100% identical to *P. chlororaphis*, which was previously described for LR1A. The LR2B sequence was also 100% identical to *P. fluorescens*, which was previously described for LR2A. The sequence was 100% identical to *P. protegens*, which was previously described for LR1B.

The LR3A sample was sequenced using the 1492r primer, which produced a high-quality sequence of 838 consecutive base pairs. This LR3A sequence was 100% identical to that of *P. fluorescens*, which was previously described for LR2A. The LR3A sequence was also 100% identical to *P. veronii*, which was previously described for LR1B. The LR3A sequence was 100% identical to *P. fildesensis*, which was previously described for LR2A.

The LR3B sample was sequenced using the 8f primer, which produced a high-quality sequence of 526 consecutive base pairs. This truncated LR3B sequence was 100% identical to *P. veronii*, which was previously described for LR1B. The LR3B sequence was also 100% identical to *P. fluorescens*, which was previously described for LR2A. The LR3B sequence was 100% identical to *P. fildesensis*, which was previously described for LR2A.

Cells collected from the streak plates for each of the three isolates were observed using epifluorescence (Appendix E). Figures 10, 11, and 12 show the cells from the LR2B sample under bright field microscopy, the blue emission filter, and the yellow emission filter respectively.

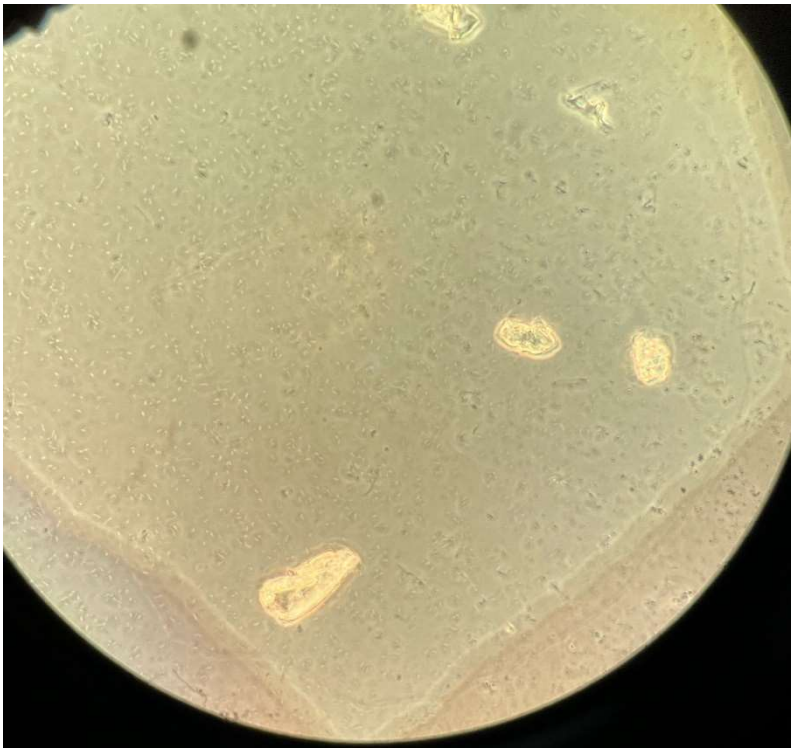

Figure 10. LR2B bright field

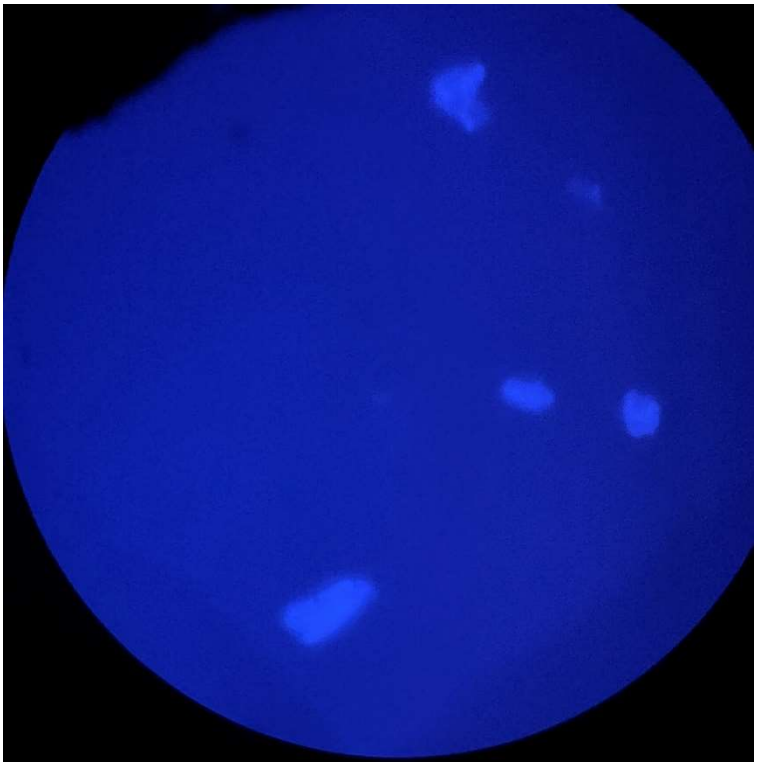

Figure 11. LR2B blue filter

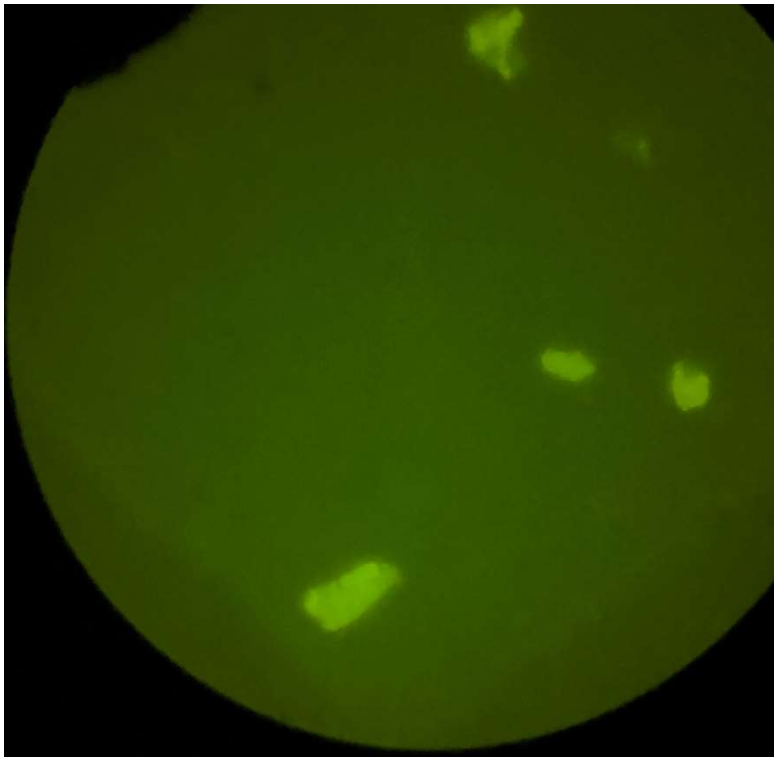

Figure 12. LR2B yellow filter

Chapter 5

Discussion and Analysis

Biofilm cells were recovered from BR (Figure 2) and LR (Figure 3), and repeated purging through a syringe needle was effective in breaking up the biofilm aggregates (Figure 3). This biofilm disruption allowed for individual cells to be sorted during flow cytometry. A greater percentage of cells from LR were isolated during flow cytometry on the basis of putative polyphosphate inclusions than from BR, but both experimental samples had over 175,000 cells recovered due to an adequate polyphosphate fluorescence relative to DNA fluorescence. This result suggests that the DAPI staining and biofilm disruption provided an adequate quantity of cells for study and that polyphosphate granules were detected in a portion of the cells taken from each rock.

The ability to recover microbial colonies from the sorted fractions (Figures 6 through 8) support the result from Terashima et al., 2020 that some microbes stained with DAPI and isolated by flow cytometry remain viable when an adequate ratio of isolated cells to PBS buffer are added; in this case 100 µL of isolated cells and no PBS buffer for LR1 and LR2 and 50 µL of isolated cells and 50 µL of PBS buffer for LR3. An acetate-based medium was used in this research with continuous aerobic incubation. With the demonstration of this technique, different media could be used to try to expand the diversity of recovered isolates.

PCR amplification of the 16S rRNA gene using primers 8f and 1492r was successful from each isolate, even using whole cells taken from the respective colony without DNA extraction and purification steps. Comparing the bands in each of the three middle lanes, which contained PCR product from LR1, LR2, and LR3 respectively, with the 1 Kb Plus DNA ladder on either side shows band lengths of approximately 1,500 base pairs (Figure 9). This is the

expected result for the amplification of the nearly full-length 16S rRNA gene using primers 8f and 1492r.

The BLAST results using the quality-trimmed sequences for LR1A, LR1B, LR2A, LR2B, LR3A, and LR3B (i.e., each isolate PCR product, sequenced from both end) suggest that each of the colonies contain members of the genus *Pseudomonas*. Based on high percentages of identical 16S rRNA gene sequences, there is a probability that the species isolated were closely related to *P. chengduensis*, *P. tolaasii*, *P. protegens*, *P. chlororaphis*, *P. veronii*, *P. extremorientalis*, *P. fluorescens*, and *P. fildesensis*. The LR1A and LR1B sequences, which are derived from the opposing ends of the same PCR products, do not share species that have the highest percentage of identical sequences. The LR2A and LR2B sequences share the species *P. fluorescens* among the highest percentage of identical sequences. Using this same measurement, the LR3A and LR3B share the species *P. fluorescens*, *P. veronii*, and *P. fildesensis*. These matches are based only on the 16S rRNA gene fragment sequences used in the BLAST analysis, and do not provide conclusive identification of the isolates. Moreover, multiple sequences had identical or very similar match percentages to the isolate sequences, which also precludes unequivocal identification. Nevertheless, the consistency of identifications makes it highly likely the isolates are a *Pseudomonas* species similar to those mentioned above.

The pairs of LR2 and LR3 samples sharing common species increases the likelihood that the results of the sequencing produced an accurate assessment of the identities of the microbes present at the selected environmental site. Of the species with a high percentage of identical sequences to the isolated microbes, *P. chlororaphis* and *P. protegens* may be PAOs due to the documented ability of phosphorus metabolism of certain *P. chlororaphis* isolates and the documentation of certain *P. protegens* isolates to have genes associated with PHA catabolism.

The results from fluorescence microscopy (Figures 10 through 12 and Figures 25 through 39 in Appendix E) show that cells from each isolate contain genetic material (blue DAPI response) and polyphosphate (yellow DAPI response). These findings suggest that each of the isolates could be PAOs. While the results are inconclusive regarding whether novel PAO isolates were recovered from the stream biofilms, it is possible the species matches identified above are capable of polyphosphate accumulation that simply has not been characterized in previous studies of these isolates. Based on the understanding of existing model PAOs, detection of this phenotype might require alternating aerobic and anaerobic conditions and microscopic or chemical inspection for intracellular polyphosphate granules, which is not a routine phenotypic test in characterizing microbial isolates.

Chapter 6

Conclusion and Future Work

The objective of this study was to apply bioprospecting in an attempt to isolate PAOs from rock biofilm samples taken from Spring Creek in Centre County, Pennsylvania. This was accomplished by using DAPI staining and flow cytometry to physically enrich prospective PAOs, culture the prospective PAOs, and use 16S rRNA gene sequencing to identify the isolates present at the selected environmental site.

Three colonies were grown from the cells isolated for polyphosphate content during flow cytometry, verifying that certain microbes remain viable after DAPI staining and flow cytometry. Gel electrophoresis following 16S rRNA gene-targeted PCR suggested that the 8f and 1492r primers successfully amplified the 16S rRNA gene. Sequencing using the 8f and 1492r primers for the LR1, LR2, and LR3 experimental samples produced sequencing results that were analyzed using BLAST to match the sequences to known microbial species.

The BLAST results indicated that it was likely the isolates belonged to the genus *Pseudomonas* and the sequences had a high percentage that was identical to the species *P. chengduensis*, *P. tolaasii*, *P. protegens*, *P. chlororaphis*, *P. veronii*, *P. extremorientalis*, *P. fluorescens*, and *P. fildesensis*. *P. chlororaphis* and *P. protegens* may be PAOs due to documented phosphorus metabolism and PHA catabolism, respectively.

The LR1A and LR1B sequences do not share species that have the highest percentage of identical sequences. The LR2A and LR2B sequences both have a high percentage of identical sequence to the species *P. fluorescens*. The LR3A and LR3B sequences both have a high percentage of identical sequence to the species *P. fluorescens*, *P. veronii*, and *P. fildesensis*. The

results of DAPI staining and fluorescence microscopy visualization suggest that each of the isolates could be PAOs due to the fluorescence of cells under the yellow filter.

Suggested future work includes further testing to determine if the isolates are PAOs by testing for further PAO traits. Testing could include giving a feed of phosphate and acetate under anaerobic conditions and seeing if they accumulate PHAs anaerobically and polyphosphate aerobically. Moreover, with the demonstrated ability of separating biofilm-growing cells and isolating DAPI-stained cells, the medium used to recover isolate from the flow cytometry sorted cell fractions could be varied to potentially retrieve microbes under alternate growth conditions. The isolates retrieved in this study could also be tested for EBPR compatibility by being introduced to a laboratory-scale EBPR reactor and measuring their impact on the efficiency of phosphate removal from the reactor.

Appendix A: Solutions Used

Table 1. Growth medium Solution A

	Total Volume (L)	0.15
Compound	**Concentration (g/L)**	**Mass (g)**
NH_4Cl	1.02	0.153
Peptone	0.010	0.0015
Yeast	0.010	0.0015
$MgSO_4*7H_2O$	1.2	0.18
$CaCl_2*H_2O$	0.19	0.029
$NaAc*3H_2O$	11.33	1.70

Table 2. Growth medium Solution B

	Total Volume (L)	0.85
Compound	**Concentration (g/L)**	**Mass (g)**
K_2HPO_4	0.132	0.112
KH_2PO_4	0.103	0.0876

Table 3. Growth medium Trace Metals

	Total Volume (L)	0.002
Compound	**Concentration (g/L)**	**Mass (g)**
$FeCl_3$	0.90	0.0018
H_3BO_3	0.15	0.00030
$CuSO_4*5H_2O$	0.030	0.000060
KI	0.18	0.00036
$MnCl_2*4H_2O$	0.12	0.00024
$Na_2MoO_4*2H_2O$	0.060	0.00012
$ZnSO_4*7H_2O$	0.12	0.00024
$CoCl_2*6H_2O$	0.15	0.00030
disodium EDTA	11.50	0.023

Table 4. Phosphate-buffered saline solution

	Total Volume (L)	0.1
Compound	**Concentration (g/L)**	**Mass (g)**
NaCl	8.0	0.8
KCl	0.2	0.02
Na_2HPO_4	1.42	0.142
KH_2PO_4	0.24	0.024

Table 5. Polymerase Chain Reaction solution

	Total Volume (µL)	0.1
Compound	**Volume/Isolate (µL)**	**Volume (µL)**
Promega PCR Master Mix	20	60
8f Primer	1.6	4.8
1492r Primer	1.6	4.8
Distilled Water	16.8	50.4

Table 6. Gel composition

Total Volume (mL)	50
Compound	**Amount**
1% Agarose (g)	0.5
Tris-acetate-EDTA (mL)	20
10,000X SYBR Safe DNA Stain (µL)	5
Distilled Water (mL)	30

Table 7. Gel buffer

Total Volume (mL)	1,000
Compound	**Volume (mL)**
1% Agarose	50
Tris-acetate-EDTA (mL)	20
Distilled Water (mL)	930

Appendix B: Streak Plating Images

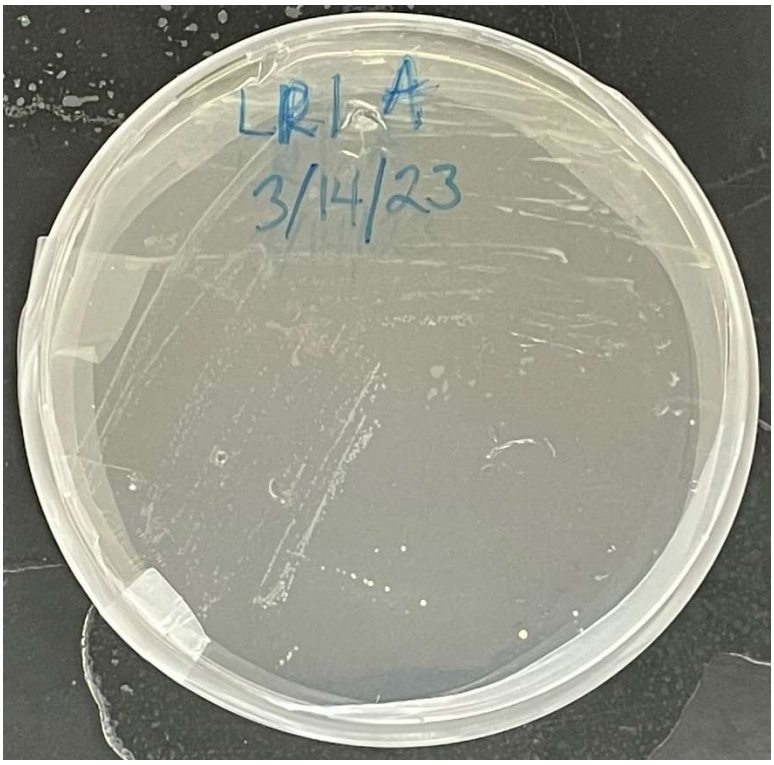

Figure 13. LR1A plate

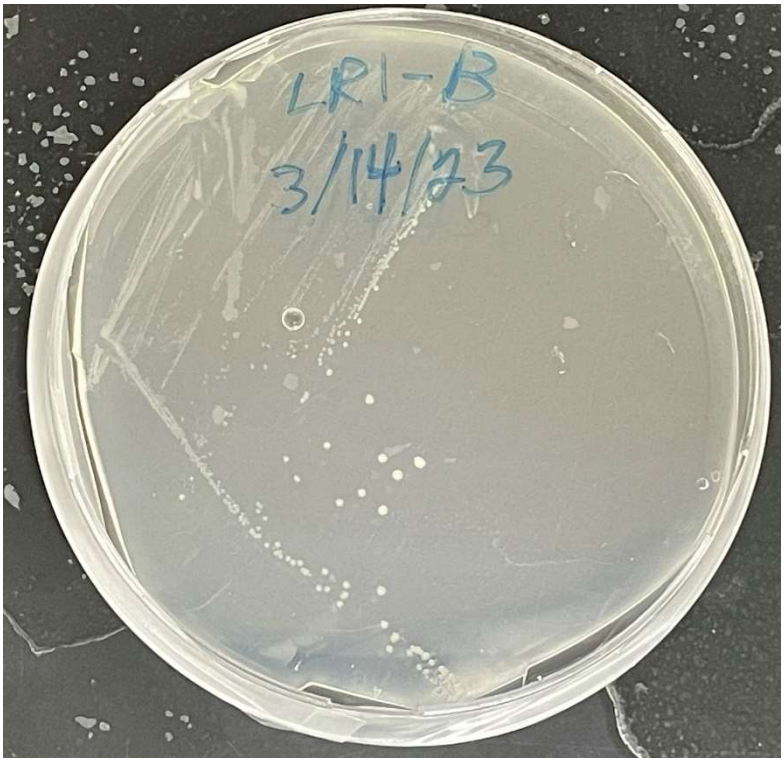

Figure 14. LR1B plate

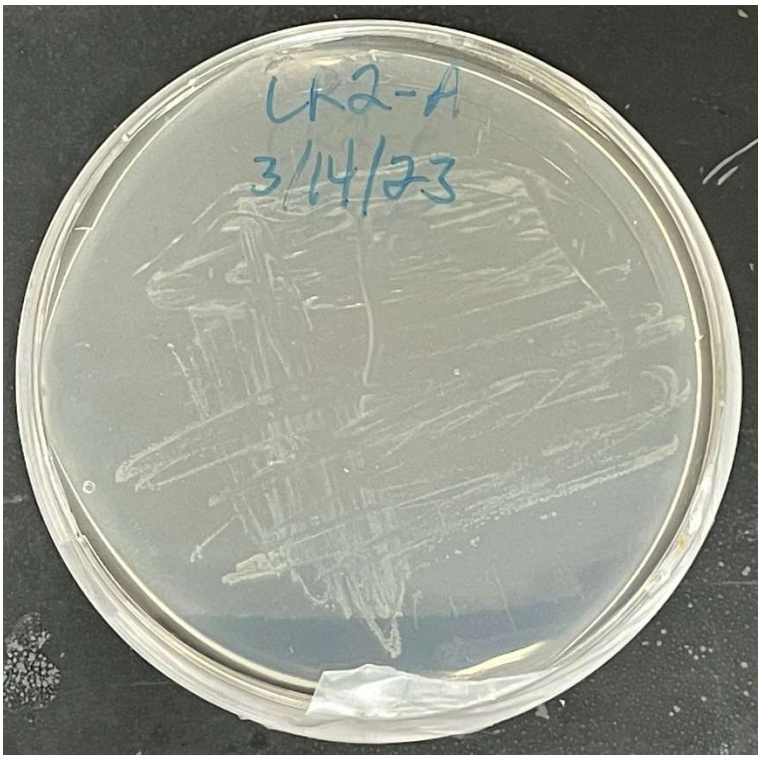

Figure 15. LR2A plate

Figure 16. LR2B plate

Figure 17. LR3A plate

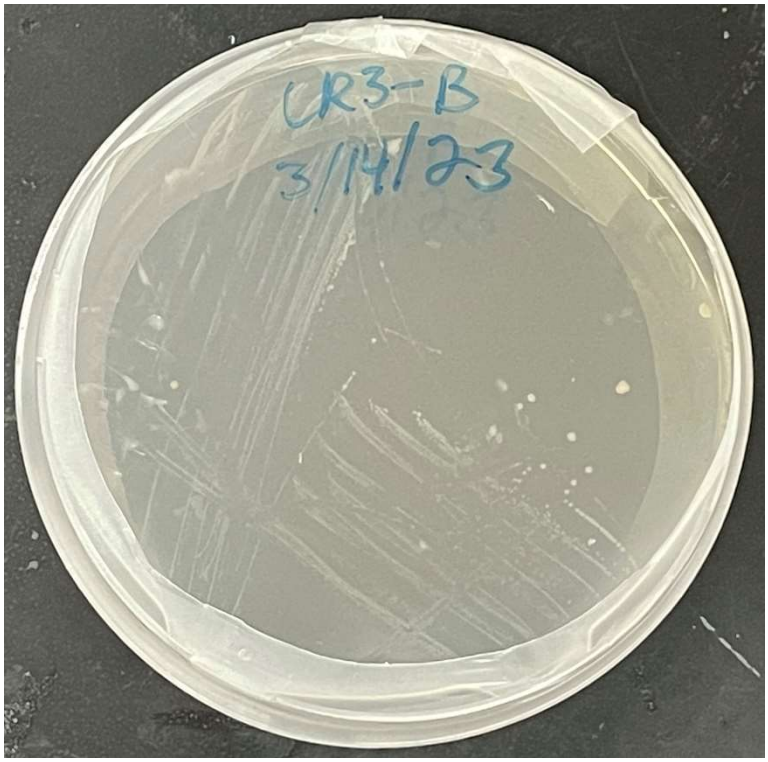

Figure 18. LR3B plate

Appendix C: Individual Sanger Sequencing Base Pair Sequences

Table 8. Sequencing results for each isolate and each primer, after quality trimming the ends

Sample	Primer	Sequence	Number of Base Pairs
LR1A	1492r	TGGGGAACGAATGCACCGTGACATTCTGATTCG CGATTACTAGCGATTCCGACTTCACGCAGTCGA TTTGCATACTGCTATCCGGAATACGATCGGTTT TATGGGATTAGCTCCACCTCGCGGCTTGGCAAC CCTCTGTACCGACCATTGAAGCGCGTGTGTAGC CCAGGCCGTAAGGGCCATGATGACTAGACGTC ATCCCCACCTTCCTCCGGTTTGTCACCGGCAGT CTCCTTAGAGTGCCCACCATAACGTGCTGGTAA CTAAGGACAAGG	275
LR1B	8f	CGGGAGGCCGCAGTGGGGAATTTTGGACAATG GGCGAAAGCCTGATCCAGCCATGCCGCGTGTG GGAAGAAGGTCTTCGGATTGTAAAGCACTTTAA GTTGGGAGGAAGGGCAGTTACCTAATACGTGA TTGTTTTGACGTTACCGACAGAATAAGCACCGG CTAACTCTGTGCCAGCATCCGCCT	186
LR2A	1492r	AGGGCCATGATGACTTGACGTCATCCCCACCTT CCTCCGGTTTGTCACCGGCAGTCTCCTTAGAGT GCCCACCATAACGTGCTGGTAACTAAGGACAA GGGTTGCGCTCGTTACGGGACTTAACCCAACAT CTCACGACACGAGCTGACGACAGCCATGCAGC ACCTGTCTCAATGTTCCCGAAGGCACCAATCTA TCTCTAGAAAGTTCATTGGATGTCAAGGCCTGG TAAGGTTCTTCGCGTTGCTTCGAATTAAACCAC ATGCTCCACCGCTTGTGCGGGCCCCCGTCAATT CATTTGAGTTTTAACCTTGCGGCCGTACTCCCC AGGCGGTCAACTTAATGCGTTAGCTGCGCCACT AAGAGCTCAAGGCTCCCAACGGCTAGTTGACA TCGTTTACGGCGTGGACTACCAGGGTATCTAAT CCTGTTTGCTCCCCACGCTTTCGCACCTCAGTGT CAGTATCAGTCCAGGTGGTCGCCTTCGCCACTG GTGTTCCTTCCTATATCTACGCATTTCACCGCTA CACAGGAAATTCCACCACCCTCTACCATACTCT AGTCAG	566
LR2B	8f	GGTGGTGGAATTTCCTGTGTAGCGGTGAAATGC GTAGATATAGGAAGGAACACCAGTGGCGAAGG CGACCACCTGGACTGATACTGACACTGAGGTGC GAAAGCGTGGGGAGCAAACAGGATTAGATACC	190

		CTGGTAGTCCACGCCGTAAACGATGTCAACTAG CCGTTGGGAGCCTTGAGCTCTTAGTGG	
LR3A	1492r	GGGCGGTGTGTACAAGGCCCGGGAACGTATTC ACCGCGACATTCTGATTCGCGATTACTAGCGAT TCCGACTTCACGCAGTCGAGTTGCAGACTGCGA TCCGGACTACGATCGGTTTTATGGGATTAGCTC CACCTCGCGGCTTGGCAACCCTCTGTACCGACC ATTGTAGCACGTGTGTAGCCCAGGCCGTAAGG GCCATGATGACTTGACGTCATCCCCACCTTCCT CCGGTTTGTCACCGGCAGTCTCCTTAGAGTGCC CACCATAACGTGCTGGTAACTAAGGACAAGGG TTGCGCTCGTTACGGGACTTAACCCAACATCTC ACGACACGAGCTGACGACAGCCATGCAGCACC TGTCTCAATGTTCCCGAAGGCACCAATCTATCT CTAGAAAGTTCATTGGATGTCAAGGCCTGGTAA GGTTCTTCGCGTTGCTTCGAATTAAACCACATG CTCCACCGCTTGTGCGGGCCCCCGTCAATTCAT TTGAGTTTTAACCTTGCGGCCGTACTCCCCAGG CGGTCAACTTAATGCGTTAGCTGCGCCACTAAG AGCTCAAGGCTCCCAACGGCTAGTTGACATCGT TTACGGCGTGGACTACCAGGGTATCTAATCCTG TTTGCTCCCCACGCTTTCGCACCTCAGTGTCAGT ATCAGTCCAGGTGGTCGCCTTCGCCACTGGTGT TCCTTCCTATATCTACGCATTTCACCGCTACACA GGAAATTCCACCACCCTCTACCATACTCTAGTC AGTCAGTTTTGAATGCAGTTCCCAGGTTGAGCC CGGGGATTTCACATCCAACTTAACTAACCACCT ACGCGCGCTTTACGC	838
LR3B	8f	TAATACGGGAGGCAGCAGTGGGGAATATTGGA CAATGGGCGAAAGCCTGATCCAGCCATGCCGC GTGTGTGAAGAAGGTCTTCGGATTGTAAAGCAC TTTAAGTTGGGAGGAAGGGCAGTTACCTAATAC GTGATTGTTTTGACGTTACCGACAGAATAAGCA CCGGCTAACTCTGTGCCAGCAGCCGCGGTAATA CAGAGGGTGCAAGCGTTAATCGGAATTACTGG GCGTAAAGCGCGCGTAGGTGGTTAGTTAAGTTG GATGTGAAATCCCCGGGCTCAACCTGGGAACT GCATTCAAAACTGACTGACTAGAGTATGGTAG AGGGTGGTGGAATTTCCTGTGTAGCGGTGAAAT GCGTAGATATAGGAAGGAACACCAGTGGCGAA GGCGACCACCTGGACTGATACTGACACTGAGG TGCGAAAGCGTGGGGAGCAAACAGGATTAGAT ACCCTGGTAGTCCACGCCGTAAACGATGTCAAC TAGCCGTTGGGAGCCTTGAGCTCTTAGTGGCGC AGCTAA	526

Appendix D: BLAST Results

Description	Scientific Name	Max Score	Total Score	Query Cover	E value	Per. Ident	Acc. Len	Accession
Pseudomonas chengduensis strain IGND-1 16S ribosomal RNA gene, par…	Pseudomo…	473	473	99%	7e-129	96.70%	1499	gi|1399601325|MH464905.1
Pseudomonas sp. BGCR2-6 16S ribosomal RNA gene, partial sequence	Pseudomo…	473	473	99%	7e-129	96.70%	682	gi|186898183|EU434628.1
Pseudomonas tolaasii strain NCPPB 741 16S ribosomal RNA gene, partia…	Pseudomo…	473	473	99%	7e-129	96.70%	1441	gi|15705394|AF320992.1
Pseudomonas sp. G11 chromosome, complete genome	Pseudomo…	467	2339	99%	4e-127	96.34%	7613543	gi|2470267714|CP120377.1
Pseudomonas sp. strain csb170 16S ribosomal RNA gene, partial sequence	Pseudomo…	467	467	99%	4e-127	96.34%	1334	gi|2461135060|OQ647875.1
Pseudomonas chlororaphis strain Rhs-P27 16S ribosomal RNA gene, part…	Pseudomo…	467	467	99%	4e-127	96.34%	1428	gi|2451843365|OQ581531.1
Pseudomonas chlororaphis strain Rhs-L4 16S ribosomal RNA gene, partia…	Pseudomo…	467	467	99%	4e-127	96.34%	1428	gi|2451843353|OQ581520.1
Pseudomonas chlororaphis strain Rhs-L21 16S ribosomal RNA gene, part…	Pseudomo…	467	467	99%	4e-127	96.34%	1426	gi|2451843351|OQ581518.1
Pseudomonas sp. strain ANT1 16S ribosomal RNA gene, partial sequence	Pseudomo…	467	467	99%	4e-127	96.34%	1405	gi|2451340902|OQ569439.1
Pseudomonas costantinii strain FHX3 16S ribosomal RNA gene, partial se…	Pseudomo…	467	467	99%	4e-127	96.34%	1439	gi|2446059277|OQ456008.1
Pseudomonas lactis strain FHX1 16S ribosomal RNA gene, partial sequen…	Pseudomo…	467	467	99%	4e-127	96.34%	1438	gi|2446059276|OQ456007.1
Pseudomonas chlororaphis strain ATCC 336631 chromosome, complete g…	Pseudomo…	467	2339	99%	4e-127	96.34%	7109352	gi|2446521677|CP118152.1
Pseudomonas chlororaphis strain ATCC 336632 chromosome, complete g…	Pseudomo…	467	2339	99%	4e-127	96.34%	7108820	gi|2446471632|CP118140.1
Pseudomonas chlororaphis subsp. aurantiaca strain GU-RS13 16S riboso…	Pseudomo…	467	467	99%	4e-127	96.34%	1438	gi|2442554727|OQ421684.1
Pseudomonas sp. TNT2022 ID1044 16S ribosomal RNA gene, partial seq…	Pseudomo…	467	467	99%	4e-127	96.34%	1537	gi|2240867244|ON555781.1
Pseudomonas azotoformans strain P36 16S ribosomal RNA gene, partial…	Pseudomo…	467	467	99%	4e-127	96.34%	1178	gi|2440439651|OQ381159.1
Pseudomonas sp. strain VITGK-10 16S ribosomal RNA gene, partial sequ…	Pseudomo…	467	467	99%	4e-127	96.34%	1499	gi|2440394421|OQ380679.1
Pseudomonas chlororaphis subsp. aureofaciens strain SF1-2 16S ribosom…	Pseudomo…	467	467	99%	4e-127	96.34%	1419	gi|2438343997|OQ363217.1
Pseudomonas sp. strain UASWS3131 CAN61 16S ribosomal RNA gene, p…	Pseudomo…	467	467	99%	4e-127	96.34%	1012	gi|2428897788|OQ283119.1
Pseudomonas sp. strain UASWS3113 CAN43 16S ribosomal RNA gene, p…	Pseudomo…	467	467	99%	4e-127	96.34%	1044	gi|2428897770|OQ283101.1
Pseudomonas sp. strain UASWS3102 CAN32 16S ribosomal RNA gene, p…	Pseudomo…	467	467	99%	4e-127	96.34%	1043	gi|2428897759|OQ283090.1
Pseudomonas lactis strain K68 16S ribosomal RNA gene, partial sequence	Pseudomo…	467	467	99%	4e-127	96.34%	1361	gi|2425700756|OQ225717.1

Figure 19. BLAST results for sample LR1A

Description	Scientific Name	Max Score	Total Score	Query Cover	E value	Per. Ident	Acc. Len	Accession
Bacterium strain AOB63 16S ribosomal RNA gene, partial sequence	bacterium	331	331	98%	3e-86	97.83%	1412	gi|2452743037|OQ601521.1
Bacterium strain AOB26 16S ribosomal RNA gene, partial sequence	bacterium	331	331	98%	3e-86	97.83%	1403	gi|2452742992|OQ601484.1
Pseudomonas protegens isolate MAG 426 chromosome, complete genome	Pseudomo…	331	1656	98%	3e-86	97.83%	6984767	gi|2457561207|CP119324.1
Anaplasma marginale isolate CVASU DPP3 16S ribosomal RNA gene, parti…	Anaplasma…	331	331	98%	3e-86	97.83%	280	gi|2452039951|OQ586446.1
Pseudomonas protegens strain N2D6 16S ribosomal RNA gene, partial seq…	Pseudomo…	331	331	98%	3e-86	97.83%	1326	gi|2451843666|OQ581753.1
Pseudomonas protegens strain N2D4 16S ribosomal RNA gene, partial seq…	Pseudomo…	331	331	98%	3e-86	97.83%	1319	gi|2451843664|OQ581752.1
Pseudomonas protegens strain Rhs0-G3 16S ribosomal RNA gene, partial …	Pseudomo…	331	331	98%	3e-86	97.83%	1410	gi|2451843367|OQ581533.1
Pseudomonas sp. strain UASWS3117 CAN47 16S ribosomal RNA gene, pa…	Pseudomo…	331	331	98%	3e-86	97.83%	1157	gi|2428897774|OQ283105.1
Pseudomonas veronii strain Yanao-Sol-15-1 16S ribosomal RNA gene, part…	Pseudomo…	331	331	98%	3e-86	97.83%	1402	gi|2428363489|OQ257001.1
Pseudomonas veronii strain Yanao-Sol-15-2 16S ribosomal RNA gene, part…	Pseudomo…	331	331	98%	3e-86	97.83%	1411	gi|2428363488|OQ257000.1
Pseudomonas veronii strain KNov-fat-3.2 16S ribosomal RNA gene, partial …	Pseudomo…	331	331	98%	3e-86	97.83%	1397	gi|2428363483|OQ256995.1
Pseudomonas syringae strain MA-70 16S ribosomal RNA gene, partial seq…	Pseudomo…	331	331	98%	3e-86	97.83%	943	gi|2425700580|OQ225584.1
Pseudomonas syringae strain MA-37 16S ribosomal RNA gene, partial seq…	Pseudomo…	331	331	98%	3e-86	97.83%	940	gi|2425700579|OQ225583.1
Pseudomonas protegens strain MA-95 16S ribosomal RNA gene, partial se…	Pseudomo…	331	331	98%	3e-86	97.83%	943	gi|2425700572|OQ225576.1
Pseudomonas protegens strain MA-85 16S ribosomal RNA gene, partial se…	Pseudomo…	331	331	98%	3e-86	97.83%	943	gi|2425700571|OQ225575.1
Pseudomonas protegens strain MA-140 16S ribosomal RNA gene, partial s…	Pseudomo…	331	331	98%	3e-86	97.83%	943	gi|2425700568|OQ225572.1
Pseudomonas protegens strain MA-130 16S ribosomal RNA gene, partial s…	Pseudomo…	331	331	98%	3e-86	97.83%	943	gi|2425700567|OQ225571.1
Pseudomonas protegens strain MA-118 16S ribosomal RNA gene, partial s…	Pseudomo…	331	331	98%	3e-86	97.83%	943	gi|2425700566|OQ225570.1
Pseudomonas sp. strain BR55 16S ribosomal RNA gene, partial sequence	Pseudomo…	331	331	98%	3e-86	97.83%	1102	gi|2425446454|OQ221821.1
Pseudomonas sp. strain BR16 16S ribosomal RNA gene, partial sequence	Pseudomo…	331	331	98%	3e-86	97.83%	1169	gi|2425446427|OQ221794.1
Pseudomonas sp. strain BR11 16S ribosomal RNA gene, partial sequence	Pseudomo…	331	331	98%	3e-86	97.83%	1136	gi|2425446423|OQ221790.1
Pseudomonas extremaustralis strain LJ41 16S ribosomal RNA gene, partia…	Pseudomo…	331	331	98%	3e-86	97.83%	1048	gi|2423348288|OQ202088.1

Figure 20. BLAST results from sample LR1B

Description	Scientific Name	Max Score	Total Score	Query Cover	E value	Per. Ident	Acc. Len	Accession
Pseudomonas extremaustralis strain WS-1 16S ribosomal RNA gene, partial seque…	Pseudomonas extremaust…	1088	1088	100%	0.0	100.00%	1463	gi|1859609919|MT641229.1
Pseudomonas sp. ADAK20 chromosome, complete genome	Pseudomonas sp. ADAK20	1088	6510	100%	0.0	100.00%	6003946	gi|1836313196|CP052858.1
Pseudomonas sp. ADAK21 chromosome, complete genome	Pseudomonas sp. ADAK21	1088	6510	100%	0.0	100.00%	6003863	gi|1836302270|CP052857.1
Pseudomonas fluorescens strain DST71 16S ribosomal RNA gene, partial sequence	Pseudomonas fluorescens	1088	1088	100%	0.0	100.00%	1470	gi|1820513021|MT186249.1
Pseudomonas veronii strain DST21 16S ribosomal RNA gene, partial sequence	Pseudomonas veronii	1088	1088	100%	0.0	100.00%	1503	gi|1820138288|MT166342.1
Pseudomonas sp. strain MWU15-20650 16S ribosomal RNA gene, partial sequence	Pseudomonas sp.	1088	1088	100%	0.0	100.00%	1528	gi|1811468846|MT101748.1
Pseudomonas sp. strain A4K089 16S ribosomal RNA gene, partial sequence	Pseudomonas sp.	1088	1088	100%	0.0	100.00%	1440	gi|1801968403|MN989123.1
Pseudomonas fluorescens strain KP-16 16S ribosomal RNA gene, partial sequence	Pseudomonas fluorescens	1088	1088	100%	0.0	100.00%	996	gi|1799195842|MN966967.1
Pseudomonas sp. DTU12.1 chromosome, complete genome	Pseudomonas sp. DTU12.1	1088	6533	100%	0.0	100.00%	5943629	gi|1796916159|CP045254.1
Pseudomonas sp. strain UASWS2116 16S ribosomal RNA gene, partial sequence	Pseudomonas sp.	1088	1088	100%	0.0	100.00%	1052	gi|1786476459|MN853680.1
Pseudomonas sp. strain RPS33 16S ribosomal RNA gene, partial sequence	Pseudomonas sp.	1088	1088	100%	0.0	100.00%	1495	gi|1785123902|MN841963.1
Pseudomonas fluorescens strain KP7 16S ribosomal RNA gene, partial sequence	Pseudomonas fluorescens	1088	1088	100%	0.0	100.00%	1298	gi|1777217792|MN715320.1
Pseudomonas sp. strain SP_20L 16S ribosomal RNA gene, partial sequence	Pseudomonas sp.	1088	1088	100%	0.0	100.00%	1262	gi|1770702559|MN624237.1
Pseudomonas veronii strain MT4 16S ribosomal RNA gene, partial sequence	Pseudomonas veronii	1088	1088	100%	0.0	100.00%	1393	gi|1739705024|MN449462.1
Pseudomonas sp. strain G11-58 16S ribosomal RNA gene, partial sequence	Pseudomonas sp.	1088	1088	100%	0.0	100.00%	1423	gi|1740674193|MN453388.1
Pseudomonas sp. G11 chromosome, complete genome	Pseudomonas sp. G11	1088	5444	100%	0.0	100.00%	7613543	gi|2470267714|CP120377.1
Pseudomonas sp. strain BILP3 16S ribosomal RNA gene, partial sequence	Pseudomonas sp.	1088	1088	100%	0.0	100.00%	1433	gi|2461130070|OQ646958.1
Pseudomonas sp. strain BIHP5 16S ribosomal RNA gene, partial sequence	Pseudomonas sp.	1088	1088	100%	0.0	100.00%	1399	gi|2461130055|OQ646943.1
Pseudomonas sp. strain UASWS3078 CAN1 16S ribosomal RNA gene, partial seq…	Pseudomonas sp.	1088	1088	100%	0.0	100.00%	1043	gi|2428897735|OQ283066.1
Pseudomonas sp. strain YG-7 16S ribosomal RNA gene, partial sequence	Pseudomonas sp.	1088	1088	100%	0.0	100.00%	992	gi|2418957229|OQ154998.1
Pseudomonas sp. strain JLS69 16S ribosomal RNA gene, partial sequence	Pseudomonas sp.	1088	1088	100%	0.0	100.00%	1394	gi|2416381906|OQ103355.1
Pseudomonas arenae strain VK110 16S ribosomal RNA, partial sequence	Pseudomonas arenae	1088	1088	100%	0.0	100.00%	1466	gi|2363086942|NR_181728.1

Figure 21. BLAST results from sample LR2A

Description	Scientific Name	Max Score	Total Score	Query Cover	E value	Per. Ident	Acc. Len	Accession
Pseudomonas sp. CBSPCAW29 chromosome, complete genome	Pseudomonas…	365	1829	100%	1e-96	100.00%	7236565	gi|2459119135|CP119371.1
Pseudomonas sp. CBSPCGW29 chromosome, complete genome	Pseudomonas…	365	1829	100%	1e-96	100.00%	7237237	gi|2459111642|CP119368.1
Pseudomonas sp. CBSPAW29 chromosome, complete genome	Pseudomonas…	365	1829	100%	1e-96	100.00%	7243675	gi|2459105190|CP119369.1
Pseudomonas sp. CBSPCBW29 chromosome, complete genome	Pseudomonas…	365	1829	100%	1e-96	100.00%	7339622	gi|2459098849|CP119370.1
Pseudomonas sp. CBSPGW29 chromosome, complete genome	Pseudomonas…	365	1829	100%	1e-96	100.00%	7237211	gi|2459092688|CP119367.1
Pseudomonas sp. CBSPBW29 chromosome, complete genome	Pseudomonas…	365	1829	100%	1e-96	100.00%	7237452	gi|2459080882|CP119366.1
Pseudomonas protegens isolate MAG 426 chromosome, complete genome	Pseudomonas…	365	1829	100%	1e-96	100.00%	6984767	gi|2457561207|CP119324.1
Pseudomonas sp. isolate MAG 425 chromosome, complete genome	Pseudomonas…	365	2195	100%	1e-96	100.00%	6914032	gi|2457505369|CP119322.1
Pseudomonas sp. IT P374 chromosome	Pseudomonas…	365	365	100%	1e-96	100.00%	5997322	gi|2449192121|CP101655.1
Pseudomonas chlororaphis strain ATCC 17411 chromosome, complete genome	Pseudomonas…	365	1829	100%	1e-96	100.00%	7212419	gi|2446618011|CP118155.1
Pseudomonas chlororaphis strain ATCC 15926 chromosome, complete genome	Pseudomonas…	365	1829	100%	1e-96	100.00%	6763921	gi|2446612011|CP118156.1
Pseudomonas chlororaphis strain ATCC 17414 chromosome, complete genome	Pseudomonas…	365	1829	100%	1e-96	100.00%	6807169	gi|2446600638|CP118154.1
Pseudomonas chlororaphis strain ATCC 17417 chromosome, complete genome	Pseudomonas…	365	1829	100%	1e-96	100.00%	6746536	gi|2446584448|CP118145.1
Pseudomonas chlororaphis strain ATCC 174152 chromosome, complete genome	Pseudomonas…	365	1829	100%	1e-96	100.00%	6664503	gi|2446578563|CP118146.1
Pseudomonas chlororaphis strain ATCC 174151 chromosome, complete genome	Pseudomonas…	365	1829	100%	1e-96	100.00%	6664157	gi|2446572677|CP118147.1
Pseudomonas chlororaphis strain ATCC 174181 chromosome, complete genome	Pseudomonas…	365	1829	100%	1e-96	100.00%	6883267	gi|2446555952|CP118144.1
Pseudomonas chlororaphis strain ATCC 174182 chromosome, complete genome	Pseudomonas…	365	1829	100%	1e-96	100.00%	6881643	gi|2446543336|CP118143.1
Pseudomonas chlororaphis strain ATCC 17809 chromosome, complete genome	Pseudomonas…	365	1463	100%	1e-96	100.00%	7020903	gi|2446534350|CP118142.1
Pseudomonas chlororaphis strain ATCC 17811 chromosome, complete genome	Pseudomonas…	365	1829	100%	1e-96	100.00%	7189114	gi|2446527964|CP118153.1
Pseudomonas chlororaphis strain ATCC 336631 chromosome, complete genome	Pseudomonas…	365	1829	100%	1e-96	100.00%	7109352	gi|2446521677|CP118152.1
Pseudomonas chlororaphis strain DSM 21509 chromosome, complete genome	Pseudomonas…	365	1829	100%	1e-96	100.00%	7064975	gi|2446515420|CP118150.1
Pseudomonas chlororaphis strain ATCC 17814 chromosome, complete genome	Pseudomonas…	365	1829	100%	1e-96	100.00%	6807913	gi|2446509353|CP118141.1

Figure 22. BLAST results from sample LR2B

Description	Scientific Name	Max Score	Total Score	Query Cover	E value	Per. Ident	Acc. Len	Accession
Pseudomonas fluorescens strain B xNS6 16S ribosomal RNA gene, partial sequence	Pseudomonas fluorescens	1611	1611	100%	0.0	100.00%	1359	gi|1821474374|MT199167.1
Pseudomonas fluorescens strain KP-16 16S ribosomal RNA gene, partial sequence	Pseudomonas fluorescens	1611	1611	100%	0.0	100.00%	996	gi|1799195842|MN966967.1
Pseudomonas fluorescens strain C01 16S ribosomal RNA gene, partial sequence	Pseudomonas fluorescens	1611	1611	100%	0.0	100.00%	1417	gi|1619085084|MK796436.1
Pseudomonas sp. strain 50_OK_6 16S ribosomal RNA gene, partial sequence	Pseudomonas sp.	1611	1611	100%	0.0	100.00%	1360	gi|1277462928|MF436694.1
Pseudomonas libanensis strain 50_OK_3 16S ribosomal RNA gene, partial sequen...	Pseudomonas libanensis	1611	1611	100%	0.0	100.00%	1329	gi|1277462926|MF436692.1
Pseudomonas fluorescens strain PF74 16S ribosomal RNA gene, partial sequence	Pseudomonas fluorescens	1611	1611	100%	0.0	100.00%	1379	gi|1240181264|MF838661.1
Pseudomonas sp. strain QBA3 16S ribosomal RNA gene, partial sequence	Pseudomonas sp.	1611	1611	100%	0.0	100.00%	1202	gi|1238388725|MF782452.1
Pseudomonas fluorescens strain L111 chromosome, complete genome	Pseudomonas fluorescens	1611	1611	100%	0.0	100.00%	6606606	gi|1057937137|CP015638.1
Pseudomonas fluorescens strain L321 chromosome, complete genome	Pseudomonas fluorescens	1611	1611	100%	0.0	100.00%	6641144	gi|1057931316|CP015637.1
Pseudomonas sp. G11 chromosome, complete genome	Pseudomonas sp. G11	1611	8059	100%	0.0	100.00%	7613543	gi|2470267714|CP120377.1
Pseudomonas veronii strain MS1 16S ribosomal RNA gene, partial sequence	Pseudomonas veronii	1611	1611	100%	0.0	100.00%	1463	gi|922590947|KT438072.1
Pseudomonas fluorescens strain KJP-1 16S ribosomal RNA gene, partial sequence	Pseudomonas fluorescens	1611	1611	100%	0.0	100.00%	1415	gi|2257448748|ON797327.1
Pseudomonas fluorescens strain AF78II14 16S ribosomal RNA gene, partial seque...	Pseudomonas fluorescens	1611	1611	100%	0.0	100.00%	1486	gi|2177429029|OM250458.1
Pseudomonas fluorescens strain AF8I4 16S ribosomal RNA gene, partial sequence	Pseudomonas fluorescens	1611	1611	100%	0.0	100.00%	1486	gi|2177429008|OM250437.1
Pseudomonas fluorescens strain CPO 4.0057 16S ribosomal RNA gene, partial seq...	Pseudomonas fluorescens	1611	1611	100%	0.0	100.00%	1189	gi|594553134|KF921604.1
Pseudomonas sp. TKP, complete genome	Pseudomonas sp. TKP	1611	8036	100%	0.0	100.00%	7012672	gi|566060467|CP006852.1
Pseudomonas sp. OVF7 16S ribosomal RNA gene, partial sequence	Pseudomonas sp. OVF7	1611	1611	100%	0.0	100.00%	1411	gi|530330265|KF498712.1
Pseudomonas fluorescens strain ECCN 10b 16S ribosomal RNA gene, partial sequ...	Pseudomonas fluorescens	1611	1611	100%	0.0	100.00%	1547	gi|1995418920|MW672582.1
Pseudomonas fluorescens strain JZ-DZ1 16S ribosomal RNA gene, partial sequence	Pseudomonas fluorescens	1611	1611	100%	0.0	100.00%	1389	gi|451778528|KC351184.1
Pseudomonas sp. JCM 5480 gene for 16S ribosomal RNA, partial sequence	Pseudomonas sp. JCM 5480	1611	1611	100%	0.0	100.00%	1459	gi|359268890|AB685685.1
Pseudomonas sp. F16a 16S ribosomal RNA gene, partial sequence	Pseudomonas sp. F16a	1611	1611	100%	0.0	100.00%	1400	gi|253741311|GQ247733.1
Pseudomonas sp. LBC1(2012) 16S ribosomal RNA gene, partial sequence	Pseudomonas sp. LBC1(2...	1609	1609	99%	0.0	100.00%	1398	gi|385152869|JN940803.1

Figure 23. BLAST results from sample LR3A

Description	Scientific Name	Max Score	Total Score	Query Cover	E value	Per. Ident	Acc. Len	Accession
Pseudomonas fluorescens strain VP5 16S ribosomal RNA gene, partial s...	Pseudomo...	1012	1012	100%	0.0	100.00%	1136	gi|459360580|KC495567.1
Pseudomonas sp. c59 16S ribosomal RNA gene, partial sequence	Pseudomo...	1012	1012	100%	0.0	100.00%	1453	gi|239829332|FJ950558.1
Pseudomonas sp. BSLX 16S ribosomal RNA gene, partial sequence	Pseudomo...	1012	1012	100%	0.0	100.00%	1400	gi|116582861|EF016111.1
Pseudomonas veronii strain M6 16S ribosomal RNA gene, partial sequence	Pseudomo...	1008	1008	99%	0.0	100.00%	1487	gi|1433393201|MH665738.1
Pseudomonas sp. BSLY 16S ribosomal RNA gene, partial sequence	Pseudomo...	1008	1008	99%	0.0	100.00%	1397	gi|116582862|EF016112.1
Pseudomonas sp. G11 chromosome, complete genome	Pseudomo...	1006	5031	99%	0.0	100.00%	7613543	gi|2470267714|CP120377.1
Pseudomonas sp. strain BWLR6 16S ribosomal RNA gene, partial seque...	Pseudomo...	1006	1006	99%	0.0	100.00%	1439	gi|2461130248|OQ647119.1
Pseudomonas sp. strain BWLB7 16S ribosomal RNA gene, partial sequen...	Pseudomo...	1006	1006	99%	0.0	100.00%	1431	gi|2461130227|OQ647098.1
Pseudomonas sp. strain BWHT2 16S ribosomal RNA gene, partial seque...	Pseudomo...	1006	1006	99%	0.0	100.00%	1431	gi|2461130219|OQ647090.1
Pseudomonas sp. strain BWHR24 16S ribosomal RNA gene, partial sequ...	Pseudomo...	1006	1006	99%	0.0	100.00%	1432	gi|2461130204|OQ647075.1
Pseudomonas sp. strain BWHR11 16S ribosomal RNA gene, partial sequ...	Pseudomo...	1006	1006	99%	0.0	100.00%	1435	gi|2461130197|OQ647068.1
Pseudomonas sp. strain BWHP26 16S ribosomal RNA gene, partial sequ...	Pseudomo...	1006	1006	99%	0.0	100.00%	1433	gi|2461130194|OQ647065.1
Pseudomonas sp. strain BWHP36 16S ribosomal RNA gene, partial sequ...	Pseudomo...	1006	1006	99%	0.0	100.00%	1432	gi|2461130185|OQ647056.1
Pseudomonas sp. strain BWLP3 16S ribosomal RNA gene, partial sequen...	Pseudomo...	1006	1006	99%	0.0	100.00%	1433	gi|2461130157|OQ647028.1
Pseudomonas sp. strain BWLP1 16S ribosomal RNA gene, partial sequen...	Pseudomo...	1006	1006	99%	0.0	100.00%	1433	gi|2461130156|OQ647027.1
Pseudomonas sp. strain BWLP14 16S ribosomal RNA gene, partial seque...	Pseudomo...	1006	1006	99%	0.0	100.00%	1432	gi|2461130152|OQ647023.1
Pseudomonas sp. strain BSLA4 16S ribosomal RNA gene, partial sequen...	Pseudomo...	1006	1006	99%	0.0	100.00%	1421	gi|2461130116|OQ646995.1
Pseudomonas sp. strain BILT1 16S ribosomal RNA gene, partial sequence	Pseudomo...	1006	1006	99%	0.0	100.00%	1429	gi|2461130084|OQ646972.1
Pseudomonas sp. strain BIHB5 16S ribosomal RNA gene, partial sequence	Pseudomo...	1006	1006	99%	0.0	100.00%	1430	gi|2461130048|OQ646936.1
Pseudomonas sp. strain LG1A 16S ribosomal RNA gene, partial sequence	Pseudomo...	1006	1006	99%	0.0	100.00%	1400	gi|2449540212|OQ517060.1
Pseudomonas veronii strain Yanao-Sol-15-1 16S ribosomal RNA gene, pa...	Pseudomo...	1006	1006	99%	0.0	100.00%	1402	gi|2428363489|OQ257001.1
Pseudomonas veronii strain Yanao-Sol-15-2 16S ribosomal RNA gene, pa...	Pseudomo...	1006	1006	99%	0.0	100.00%	1411	gi|2428363488|OQ257000.1

Figure 24. BLAST results from sample LR3B

Appendix E: Fluorescence Microscopy Results

Figure 25. LR1A bright field

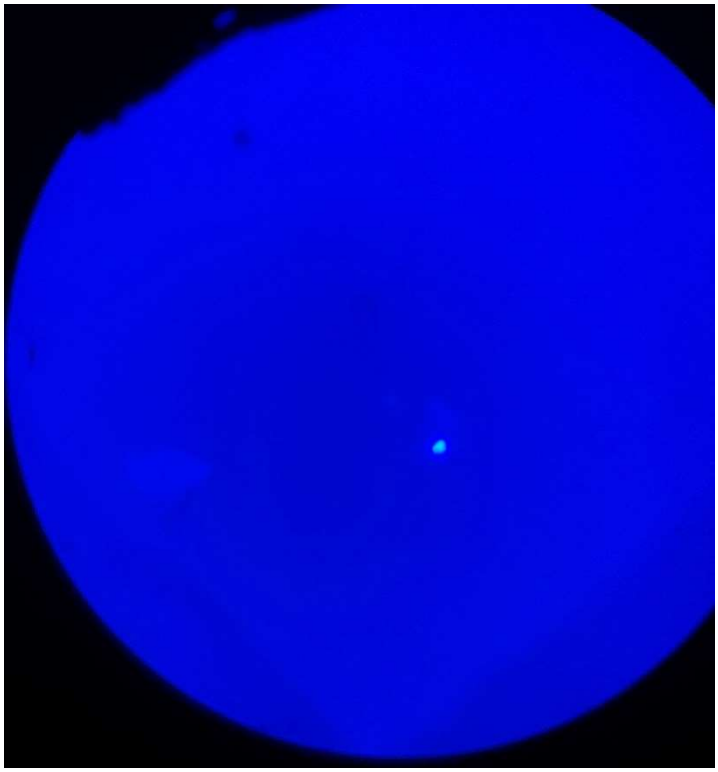

Figure 26. LR1A blue filter

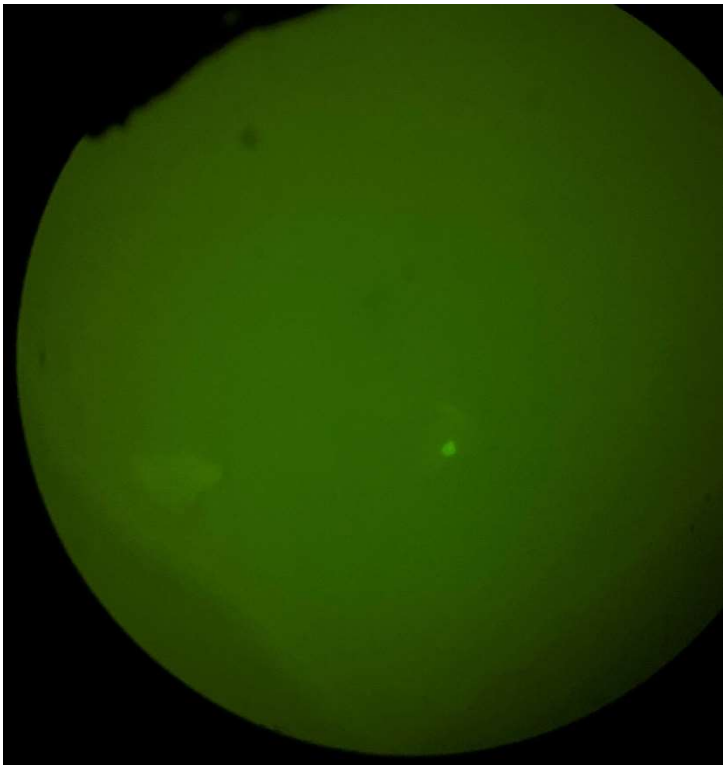

Figure 27. LR1A yellow filter

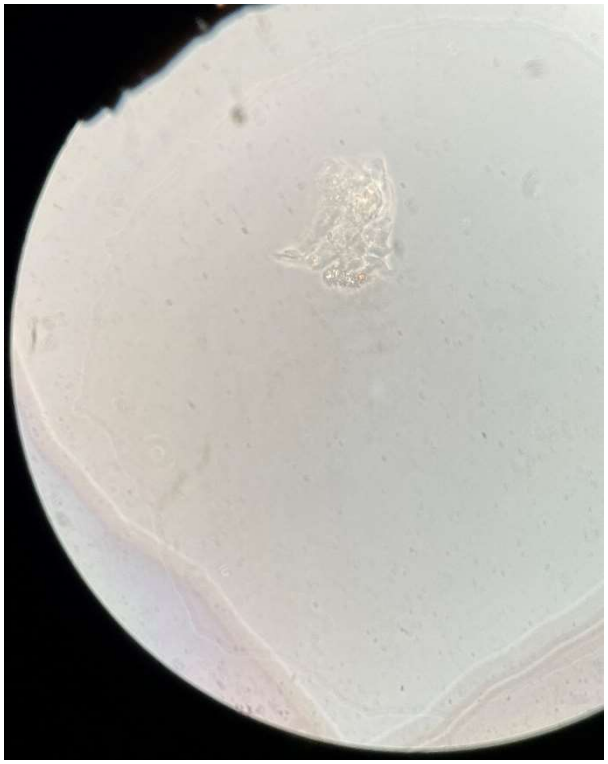

Figure 28. LR1B bright field

Figure 29. LR1B blue filter

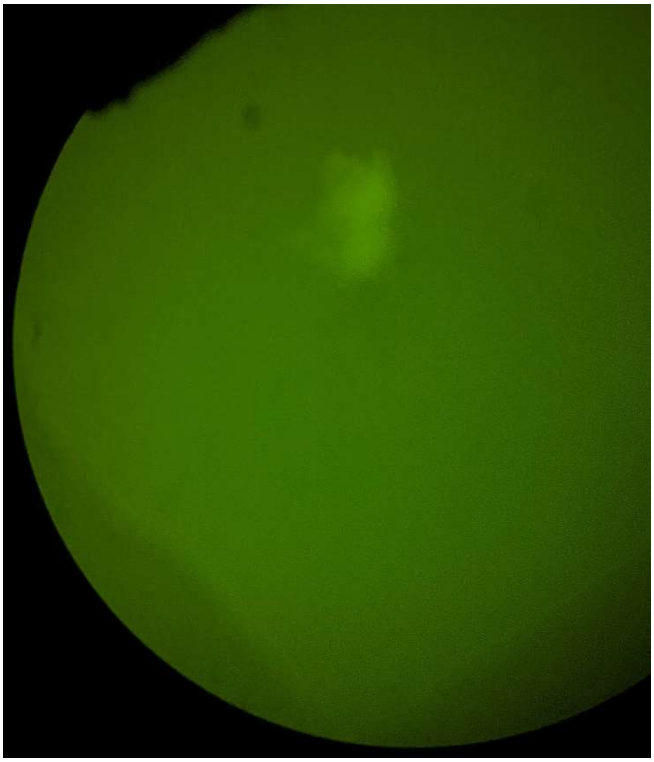

Figure 30. LR1B yellow filter

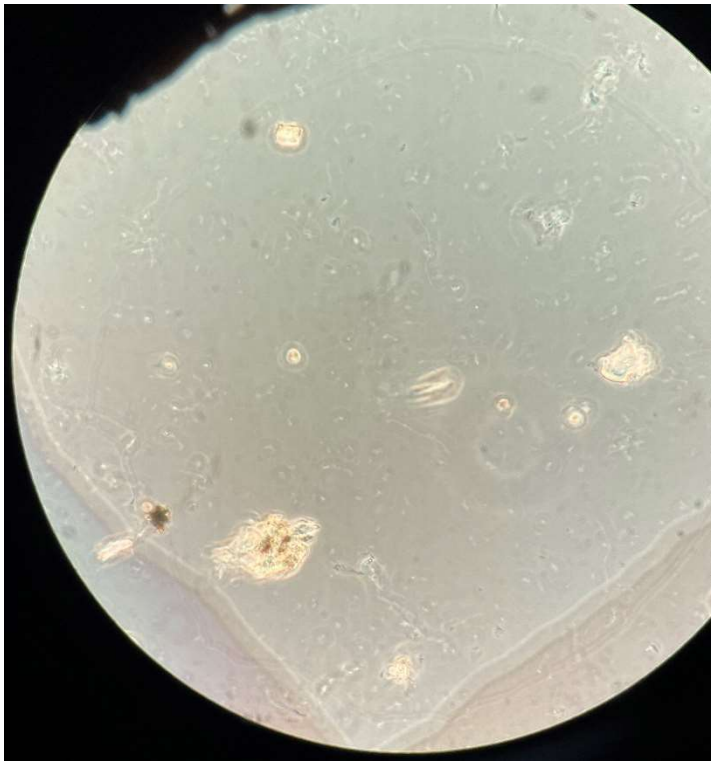

Figure 31. LR2A bright field

Figure 32. LR2A blue filter

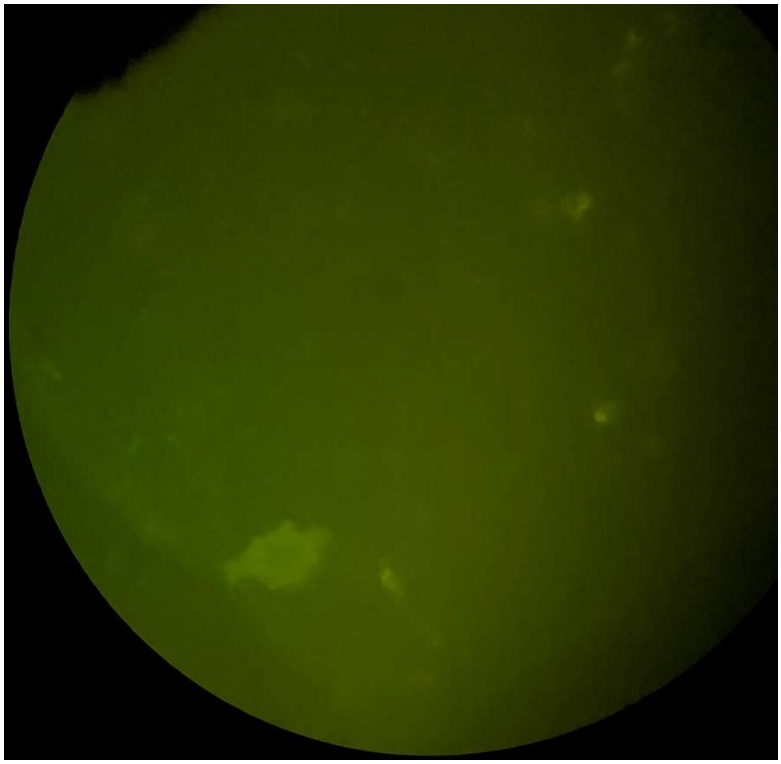

Figure 33. LR2A yellow filter

Figure 34. LR3A bright field

Figure 35. LR3A blue filter

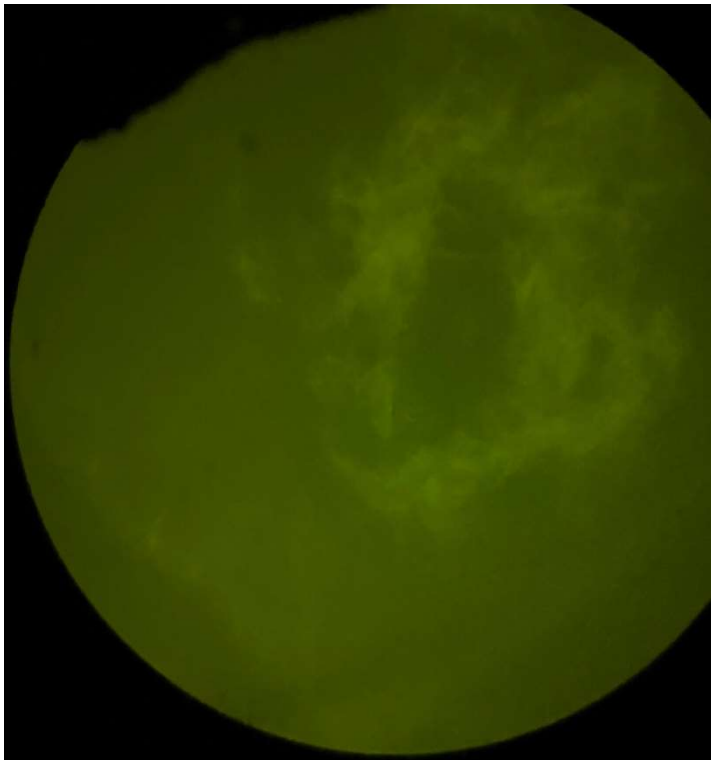

Figure 36. LR3A yellow filter

Figure 37. LR3B bright field

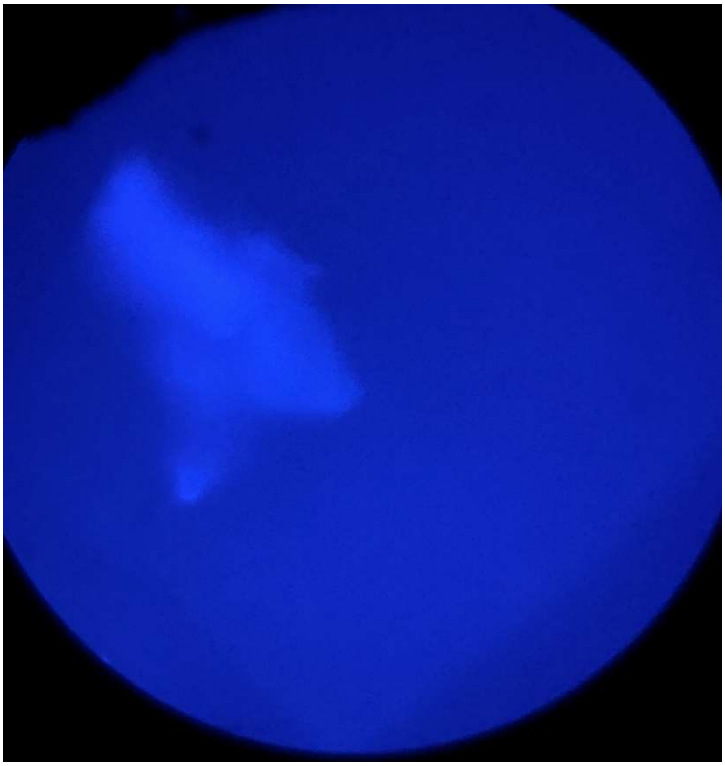

Figure 38. LR3B blue filter

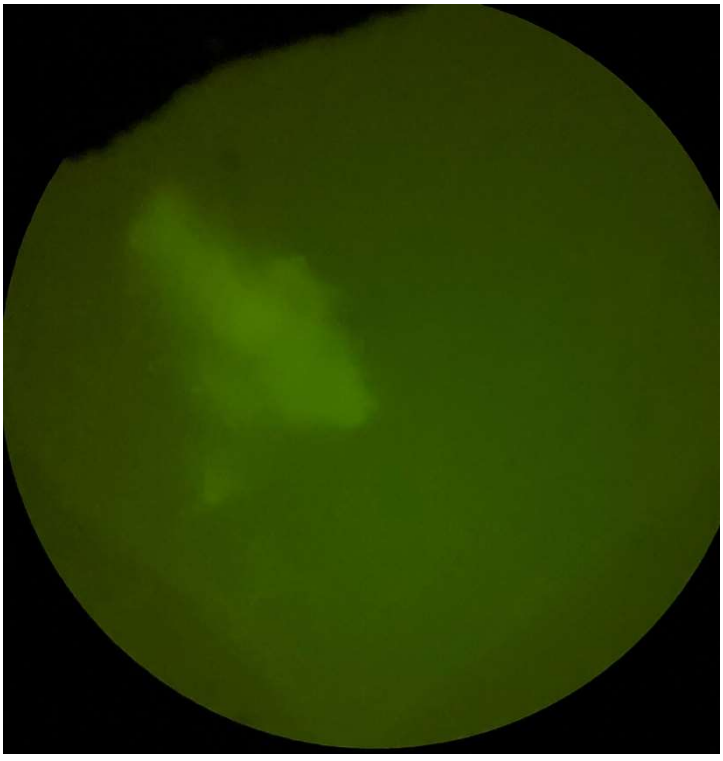

Figure 39. LR3B yellow filter

BIBLIOGRAPHY

Anderson, A. J., & Kim, Y. C. (2020). Insights into Plant-beneficial Traits of Probiotic Pseudomonas chlororaphis Isolates. *Journal of Medical Microbiology*, *69*(3). https://doi.org/10.1099/jmm.0.001157

Chislock, M. F., Doster, E., Zitomer, R. A. & Wilson, A. E. (2013) Eutrophication: Causes, Consequences, and Controls in Aquatic Ecosystems. *Nature Education Knowledge* 4(4):10

Cordell, D., & White, S. (2011). Peak Phosphorus: Clarifying the Key Issues of a Vigorous Debate About Long-term Phosphorus Security. *Sustainability*, *3*(10), 2027–2049. https://doi.org/10.3390/su3102027

Elomari, M., Coroler, L., Hoste, B., Gillis, M., Izard, D., & Leclerc, H. (1996). DNA relatedness among pseudomonas strains isolated from natural mineral waters and proposal of pseudomonas veronii sp. nov.. *International Journal of Systematic Bacteriology*, *46*(4). https://doi.org/10.1099/00207713-46-4-1138

Gobler, C. J. (2020). Climate Change and Harmful Algal Blooms: Insights and Perspective. *Harmful Algae*, *91*. https://doi.org/10.1016/j.hal.2019.101731

Godfrey, S. A. C., Marshall, J. W., & Klena, J. D. (2001). Genetic Characterization of Pseudomonas 'NZI7' - a Novel Pathogen that Results in a Brown Blotch Disease of Agaricus bisporus. *Journal of Applied Microbiology*, *91*(3), 412–420. https://doi.org/10.1046/j.1365-2672.2001.01398.x

Günther, S. (2011). *Population Structure and Dynamics of Polyphosphate Accumulating Organisms in a Communal Wastewater Treatment Plant* (dissertation).

Ivanova, E. P., Gorshkova, N. M., Sawabe, T., Hayashi, K., Kalinovskaya, N. I., Lysenko, A. M., Zhukova, N. V., Nicolau, D. V., Kuznetsova, T. A., Mikhailov, V. V., & Christen, R.

(2002). Pseudomonas extremorientalis sp. nov., isolated from a drinking water reservoir. *International Journal of Systematic and Evolutionary Microbiology*, *52*(6). https://doi.org/10.1099/00207713-52-6-2113

Jasinski, S. M. (2011). Potash. *Society of Mining Engineering*, *63*(6), 91–92.

Johnson, J. S., Spakowicz, D. J., Hong, B.-Y., Petersen, L. M., Demkowicz, P., Chen, L., Leopold, S. R., Hanson, B. M., Agresta, H. O., Gerstein, M., Sodergren, E., & Weinstock, G. M. (2019). Evaluation of 16S rRNA Gene Sequencing for Species and Strain-level Microbiome Analysis. *Nature Communications*, *10*. https://doi.org/10.1038/s41467-019-13036-1

Lu, H., Oehmen, A., Virdis, B., Keller, J., & Yuan, Z. (2006). Obtaining Highly Enriched Cultures of Candidatus Accumulibacter Phosphates Through Alternating Carbon Sources. *Water Research*, *40*(20), 3838–3848. https://doi.org/10.1016/j.watres.2006.09.004

Luo, Y., Lei, H., Wang, R., Zhao, H., Zhang, G., & Song, C. (2021). A novel in vivo functional screening method for the candidate polyphosphate accumulating organisms isolation. *Applied Biochemistry and Microbiology*, *57*. https://doi.org/10.1134/s0003683821100045

Meng, Q., Zeng, W., Wang, B., Fan, Z., & Peng, Y. (2020). New Insights in the Competition of Polyphosphate-accumulating Organisms and Glycogen-accumulating Organisms Under Glycogen Accumulating Metabolism with Trace poly-P Using Flow Cytometry. *Chemical Engineering Journal*, *385*. https://doi.org/10.1016/j.cej.2019.123915

Nedelciu, C. E., Ragnarsdottir, K. V., Schlyter, P., & Stjernquist, I. (2020). Global Phosphorus Supply Chain Dynamics: Assessing Regional Impact to 2050. *Global Food Security*, *26*. https://doi.org/10.1016/j.gfs.2020.100426

Nielsen, P. H., McIlroy, S. J., Albertsen, M., & Nierychlo, M. (2019). Re-evaluating the Microbiology of the Enhanced Biological Phosphorus Removal Process. *Current Opinion in Biotechnology*, *57*, 111–118. https://doi.org/10.1016/j.copbio.2019.03.008

Oehman, A., Lemos, P. C., Carvalho, G., Yuan, Z., Keller, J., Blackall, L. L., & Reis, M. A. M. (2007). Advances in Enhanced Biological Phosphorus Removal: From Micro to Macro Scale. *Water Research*, *41*(11), 2271–2300. https://doi.org/10.1016/j.watres.2007.02.030

Pavlov, M. S., Lira, F., Martinez, J. L., Olivares-Pacheco, J., & Marshall, S. H. (2020). Pseudomonas fildesensis sp. nov., a Psychrotolerant Bacterium Isolated from Antarctic Soil of King George Island, South Shetland Islands. *International Journal of Systematic and Evolutionary Microbiology*, *70*(5). https://doi.org/10.1099/ijsem.0.004165

Rhodes, M. E. (1959). The Characterization of Pseudomonas fluorescens. *Journal of General Microbiology*, *21*(1). https://doi.org/10.1099/00221287-21-1-221

Rodríguez, C. A. D., Díaz-García, L., Bunk, B., Spröer, C., Herrera, K., Tarazona, N. A., Rodriguez-R, L. M., Overmann, J., & Jiménez, D. J. (2022). Novel Bacterial Taxa in a Minimal Lignocellulolytic Consortium and Their Potential for Lignin and Plastics Transformation. *ISME Communications*, *2*. https://doi.org/10.1038/s43705-022-00176-7

Tao, Y., Zhou, Y., He, X., Hu, X., & Li, D. (2014). Pseudomonas chengduensis sp. nov., Isolated from Landfill Leachate. *International Journal of Systematic and Evolutionary Microbiology*, *64*(Pt_1). https://doi.org/10.1099/ijs.0.050294-0

Tarayre, C., Nguyen, H. T., Brognaux, A., Delepierre, A., De Clercq, L., Charlier, R., Michels, E., Meers, E., & Delvigne, F. (2016). Characterisation of Phosphate Accumulating Organisms and Techniques for Polyphosphate Detection: A Review. *Sensors (Basel, Switzerland)*, *16*(6), 797. https://doi.org/10.3390/s16060797

Terashima, M., Kamagata, Y., & Kato, S. (2020). Rapid enrichment and isolation of polyphosphate-accumulating organisms through 4'6-diamidino-2-phenylindole (DAPI) staining with fluorescence-activated cell sorting (FACS). *Frontiers in Microbiology*, *11*. https://doi.org/10.3389/fmicb.2020.00793

United States Environmental Protection Agency. (2022, December 15). *Climate Change and Harmful Algal Blooms*. EPA. Retrieved April 2, 2023, from https://www.epa.gov/nutrientpollution/climate-change-and-harmful-algal-blooms

Yuan, Z., Pratt, S., & Batstone, D. J. (2012). Phosphorus Recovery from Wastewater Through Microbial Processes. *Current Opinion in Biotechnology*, *23*(6), 878–883. https://doi.org/10.1016/j.copbio.2012.08.001

ACADEMIC VITA

Gabriel C. Hiestand

EDUCATION

Bachelor of Science in Environmental Systems Engineering | Minor in Watersheds and Water Resources
College of Earth and Mineral Sciences | Schreyer Honors College
The Pennsylvania State University, University Park, PA Anticipated Graduation: May 2023

WORK EXPERIENCE

Engineering Intern McCormick & Company, Inc. June-August 2022

- Optimized water use systems at Flavor Manufacturing Center to save an estimated 6.2 million gallons of water and $144k in OPEX annually
- Streamlined sustainability data reporting and produced strategies to reach sustainability goals
- Expanded Hunt Valley Manufacturing Plant ergonomics for spice drum dumping safety

RESEARCH EXPERIENCE

Research Intern Penn State University Department of Energy and Mineral Engineering May 2021 – July 2021

- Used mathematical modeling on MATLAB software to study the impact of light intensity on the removal of ammonia from municipal wastewater treatment plants
- Developed literacy in mathematical modeling and wastewater treatment via a literature review
- Communicated results to a panel of faculty, industry professionals, and fellow interns via a recorded lightning talk, construction of a research poster, and participation in a virtual research showcase

LEADERSHIP & INVOLVEMENT

President Penn State Engineers Without Borders April 2022 – Present

- Responsible for overseeing all chapter operations, devising chapter strategy, and leading meetings
- Ambassador of the chapter across the university, among other chapters, and to alumni and partners
- Oversee ethical decisions made for served communities and that officers receive equitable resources

Project Lead Penn State Engineers Without Borders March 2021 – April 2022

- Used hydrogeological survey results to select a drilling site for a borehole that produces water for drinking, cooking, and sanitation to the 2,000 residents of Namutamba, Uganda and is projected to exceed community demand
- Successfully led the design of a greywater filtration system to completion that provides water for gardening at a school of 230 girls in Hyderabad, India
- Responsible for project documents, leading project design, and selecting a diverse team of sub-leads

HONORS

Dean's List obtained during six of seven semesters attending Penn State

Laureate of Penn State Earth and Mineral Sciences Academy for Global Experience Awarded November 2022

Recipient of the Penn State Earth and Mineral Sci. Matthew J. Wilson Honors Scholarship 2019-2021 and 2022-2023

Recipient of the McCormick US Scholarship Award 2020-2021, 2021-2022, and 2022-2023

Recipient of the Chevron Corporation Environmental Health and Safety Scholarship 2020-2021 and 2021-2022

APPLICABLE SKILLS

MATLAB | Microsoft Office | Public Speaking – National Speech and Debate Association Alumni